



J C M M

**The relationship between water vapour
imagery and thunderstorms**

Nigel M Roberts

February 2000

INTERNAL REPORT NO.110

NWP Technical Report No.300



Joint Centre for Mesoscale Meteorology

**The relationship between water vapour imagery and
thunderstorms**

Nigel M Roberts

JCMM, UK Met Office

February 2000

Contents

1.	Introduction	2
2.	Examples of thunderstorm events related to water vapour imagery	3
2.1	Dry eye thunderstorms	3
2.1.1	Advection and descent of low- θ_w air from higher latitudes	4
2.1.2	Generation of potential instability	5
2.1.3	Ascent ahead of an upper-level vorticity anomaly	6
2.1.4	Warm advection and surface heating	7
2.1.5	A summary picture	7
2.2	Dry edge thunderstorms	8
2.2.1	The large-scale trough pattern	11
2.2.2	Smaller-scale vorticity anomalies	11
2.3	Inner crescent rim thunderstorms	12
2.3.1	Why the inner edge of a crescent shaped dry intrusion?	16
2.4	Dry tip thunderstorms	18
2.4.1	Why the 'dry tip category'?	19
2.5	Warm plume thunderstorms	19
2.6	Orographic triggering at a coastal mountain barrier	21
2.7	A summary	22
3.	A study of the relationship between water vapour imagery and thunderstorms	23
3.1	The study	23
3.1.1	Possible criticism	25
3.2	Results from the summer study	25
3.2.1	Summer period storm cluster duration	26
3.2.2	Summer period storm cluster severity	28
3.3	Results from the autumn study	29
3.3.1	Autumn period storm cluster duration	30
3.3.2	Autumn period storm cluster severity	32
3.4	Combined results	33
3.4.1	Classification of the relationship to water vapour imagery	33
3.4.2	Storm cluster duration	34
3.4.3	Key results from the combined study	35
4.	Conclusions	36
5.	Acknowledgements	39
6.	References	39

1. Introduction

Mid-latitude thunderstorms are often difficult to predict, even just a few hours ahead. Usually, the area that is generally favourable for storm development is known, but to be more precise about where and when thunderstorms will break out can be a big problem. Many factors play a role and add to the complexity. A list of some of these factors includes; variations in orography, the urban heat island effect, sea breeze fronts, humidity variations, low-level convergence, gust fronts and mesoscale or synoptic scale dynamical forcing. This report concentrates primarily on one aspect, the dynamical forcing and temperature and humidity structure associated with upper/middle level vorticity anomalies that can be identified in water vapour (WV) imagery (Browning 1993, Roberts 2000). It has been noted from a variety of case studies that thunderstorms can be found within and on the edges of dry regions in WV imagery. Studies that show this relationship can be found by referencing Carr and Millard (1985), Young et al (1987), Hobbs et al (1990), Browning and Golding (1995), Browning and Roberts (1994), Roberts (1995), Browning et al (1996). These case studies focus specifically on cyclogenesis or split front events (Browning and Monk 1982). The aim here is to show greater generality in the relationship between WV dry regions and the triggering of thunderstorms; firstly, by showing several good examples and then by presenting the results of a study of over three hundred events to show just how common this relationship is. JCOMM report 109 (Roberts 2000) provides a useful background to this report, particularly in the interpretation of WV imagery.

In section 2 the set of examples will be presented which show how thunderstorm development can be linked to favourable patterns in WV imagery. Each case will be placed into one of six categories, 'dry eye', dry edge', 'inner crescent rim', dry tip, 'warm plume' and 'orographic & dry strip'. An explanation of a probable mechanism will be given for each of the categories. Thunderstorms have been located by using the UK Met Office ATD system for detecting lightning strokes (sferics) (Lee, 1989).

In section 3 the results from the study will be presented. The relationship between thunderstorm clusters and 'dark zones' in WV imagery was assessed for all significant thunderstorm events over Western Europe and the North Atlantic during summer and autumn periods in 1998.

In section 4 the conclusions are presented.

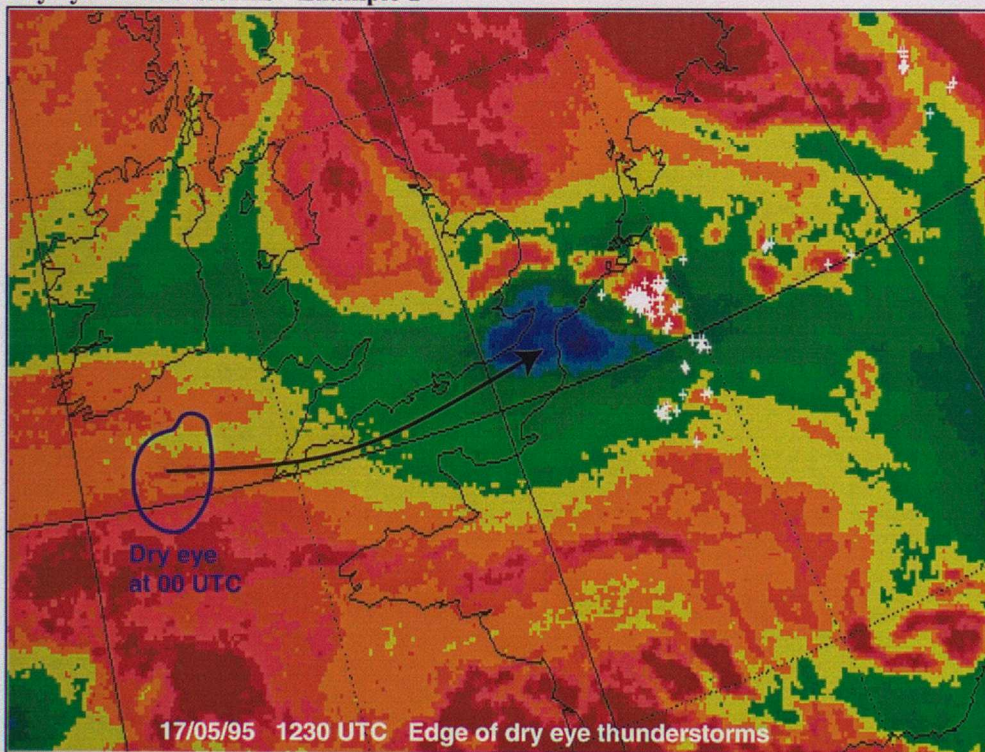
2. Examples of thunderstorm events related to WV imagery

2.1 Dry eye thunderstorms

Dry eye thunderstorms occur ahead of upper-level potential vorticity (PV) anomalies, observed in WV imagery as circular or lens shaped dry regions (see Hoskins et al 1985 about PV). These features are usually mesoscale in size ~50 - 500km across. The triggering of thunderstorms ahead of dry eye features results from a combination of some or all of four conditions being fulfilled. These are listed below and will be discussed in turn after the examples.

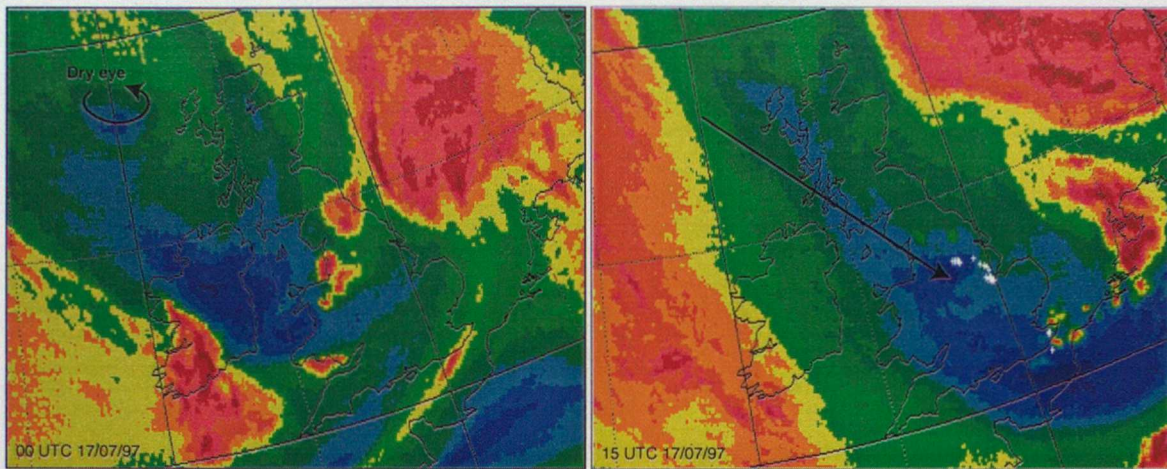
- Advection and descent of low- θ_w air from higher latitudes.
- Generation of potential instability.
- Ascent ahead of an upper-level vorticity anomaly.
- Warm advection or surface heating

Dry eye thunderstorms - Example 1



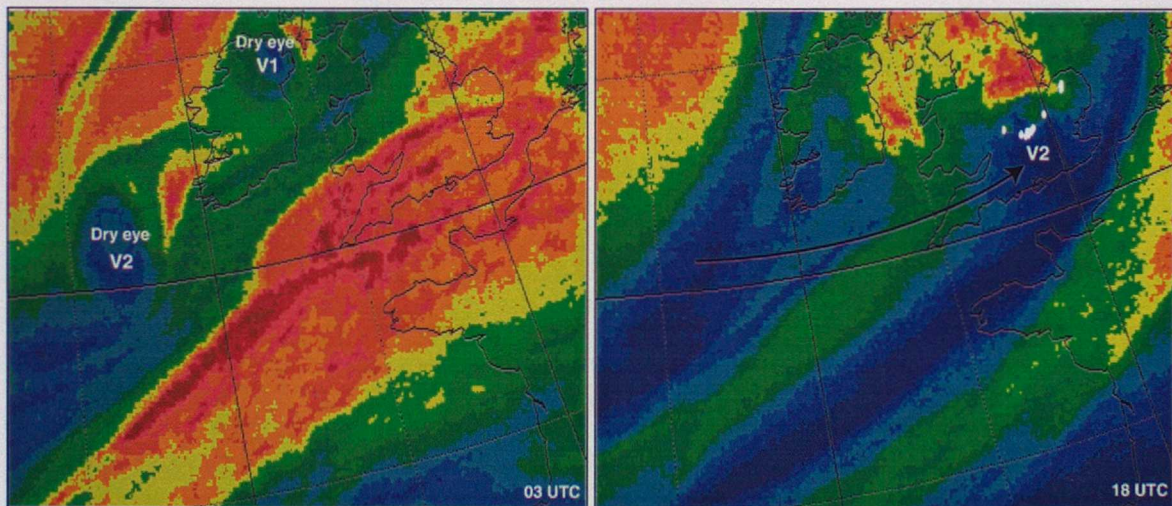
Water vapour image for 1230UTC 17/05/95. Colour transition is from driest/warmest regions shaded blue through to moist/cloudy regions shaded orange and pink. White crosses show sferics over a 40-minute interval centered at the time of the image. A dry eye traveled along the south coast of England and then into the Low Countries. An arc of thunderstorms broke out ahead of the dry eye over France, Belgium and the Netherlands from midday onwards. A diagnostic study of this case has been documented by Browning et al (1996) and a more theoretical study using a PV modification technique has been presented by Griffiths et al (1999).

Dry eye thunderstorms - Example 2



WV imagery using the same colour convention as example 1. White crosses show sferics over a 30-minute interval. Small dry eye on the tail of a larger dry intrusion traveled southeast and thunderstorms broke out ahead in an arc over eastern England from midday onwards on 17/07/97. This event was poorly forecast by the UK Met Office Limited Area Model.

Dry eye thunderstorms - Example 3



WV imagery using the same colour convention as example 1. White crosses show sferics over a 30-minute period. Two dry eye upper-level vortices were observed on 5/9/97. The first dry eye (V1) triggered thunderstorms over the North Sea and Norway from midday onwards. The second dry eye (V2) triggered thunderstorms over England in the evening as shown in the second picture. This event was poorly forecast.

2.1.1 Advection and descent of low- θ_w air from higher latitudes

If convection is to occur, potential instability is a necessity. A way of generating potential instability is by the process of differential advection of low- θ_w air over high- θ_w air (Browning et al 1996). Before differential advection in the vertical can lead to potential instability there must be differential advection in the horizontal first to create a gradient of θ_w across which the vertical shear can act. In other words, air characterised by low θ_w must be transported into a region where it will be adjacent to air with a higher θ_w (or visa versa). The existence of a dry eye, by its very

nature, shows that this has happened because the locally lower tropopause reflects the fact that the air has arrived from a higher latitude and is locally colder in the mid troposphere than the surrounding air. The upper-level vorticity associated with a dry eye can also act to transport air equatorwards behind the vortex.

The larger the difference in θ_w between air advected with a dry eye and the surrounding air, the more intense any convection is likely to be. Several factors play a part in determining the magnitude of this θ_w difference. The origin of a dry eye and where it ends up are crucial - the colder the region the dry eye associated air comes from and the warmer the region it gets to, the greater the θ_w difference. A dry eye that is embedded within a larger scale extended trough system is more likely to be connected to a feed of air from higher latitudes and get to lower latitudes than if the flow is more zonal. On the other hand, if an upper level vortex associated with an extending trough becomes isolated, it loses any new supply of cold air.

An additional and vital component is the descent of the low- θ_w air, either on the large scale along sloping isentropic surfaces or in a more concentrated region behind the upper-level vorticity anomaly. The descent acts to create a stable layer (see Figure 1) which later prevents the premature release of the potential instability generated by the process of differential advection at different levels.

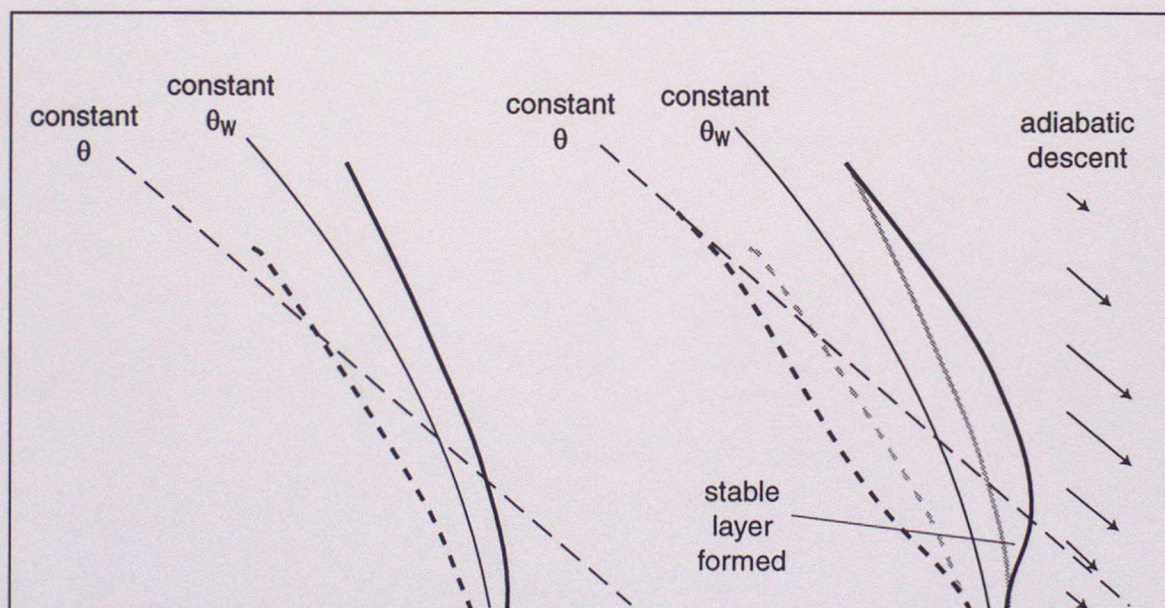


Figure 1. Schematic of atmospheric profiles of uniform wet-bulb potential temperature before and after a period of dry adiabatic descent maximised at middle levels. A result of the subsidence is the formation of a more stable layer in temperature below the level of maximum descent.

2.1.2 Generation of potential instability

Once a horizontal θ_w gradient exists, a wind shear in the vertical can act to generate potential instability. Differential advection in the vertical of θ_w surfaces can lead to overrunning of low- θ_w air over high- θ_w air. Browning et al (1996) in a study of the case in example 1 revealed this process occurring below and to the south of the dry eye. They used the UK Met Office Limited Area Model to show how the 9°C θ_w surface at 700hPa overran the same θ_w surface at 900hPa. Figure 2 is a part of a figure from that paper. Griffiths et al (1999) went a stage further with the

same case study. They used the UK Met Office mesoscale model to calculate the rate of generation of potential instability in the vicinity of the tropopause lowering: they then used a PV surgery and inversion technique to remove the upper level PV and re-calculate the rate of generation of potential instability. It was shown that for this case the upper-level PV anomaly associated with the tropopause lowering made a significant, but not total, contribution to the potential destabilisation of the atmosphere between 900 and 700hPa.

A simple westerly flow increasing with height in the absence of a vorticity anomaly could also act to generate potential instability. The upper-level PV anomaly in example 1 occurred within a larger scale trough with associated tropopause shelf and westerly jet increasing with height (see the green strip extending through Ireland to France). This may be one reason why the tropopause depression associated with the dry eye in example 1 was not responsible for as much of the potential instability as might be expected. However, although a simple westerly flow could act to make the atmosphere potentially unstable; a steady state westerly flow would not allow the differential horizontal advection that is required for the appropriate starting conditions of a θ_w gradient along the direction of the flow. At some stage in the evolution of the flow a perturbation which may be a larger scale trough or a small-scale vorticity anomaly is required to create the cross-flow θ_w gradient.

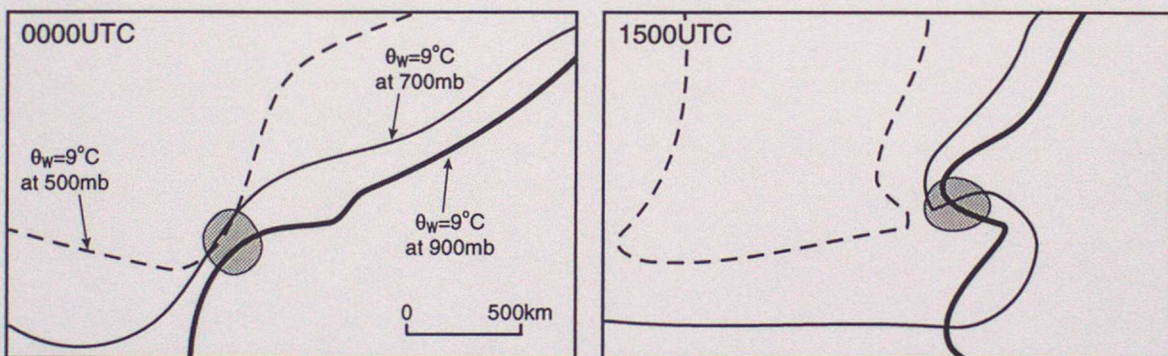


Figure 2. Selected model diagnostics showing the effect of a mesoscale vortex on the three-dimensional structure of the 9°C wet-bulb potential temperature surface. Contours show the surface at 900hPa (thin line), 700hPa (thick line) and 500hPa (dashed line) at 0000 and 1500 UTC on 17 May 1995. The shaded region shows the mesoscale vortex centre at 700hPa ($>16 \times 10^{-5} \text{s}^{-1}$ at 0000 UTC and $>22 \times 10^{-5} \text{s}^{-1}$ at 1500 UTC). Taken from Browning, Roberts & Sim (1996).

2.1.3 Ascent ahead of the upper-level vorticity anomaly

Ascent ahead of an upper-level vorticity anomaly often plays a key role in creating an environment favourable for convection to be triggered. This ascent can lead to convective triggering if:

- 1) The column of air is potentially unstable.
- 2) The higher- θ_w air at low levels is separated from the lower- θ_w air above by a stable layer; otherwise convection can be triggered without the need for dynamical ascent. Descent should have previously occurred at middle/upper levels.
- 3) There is sufficient moisture and instability at low levels to make it possible for air parcels that either freely ascend or are forced to ascend to reach saturation.

4) The ascent is strong enough to enable saturated air parcels below the stable layer to become buoyant at and above the level of the stable layer.

2.1.4 Warm advection and surface heating

Solar heating can act to increase the θ_w of the air near the surface if there is sufficient moisture. This in turn will lead to an increase in potential instability and a reduction in the amount of ascent required to release that potential instability. The reason the thunderstorms developed when and where they did in all three examples is probably because of the combination of forced ascent ahead of the dry eye and surface heating over land in the afternoon.

Low-level warm advection can also act to increase the potential instability and enhance the forced vertical motion. The phase relationship between a low-level warm tongue of air and the upper-level PV anomaly is crucial. A low-level warm tongue ahead of a dry eye is most conducive to deep large-scale ascent that may lead to convective triggering and even cyclogenesis.

2.1.5 A summary picture

The schematic in Figure 3 puts together the mechanisms outlined above. From a WV imagery perspective, a dry eye indicates the existence of an upper level vorticity anomaly, an associated vertical motion dipole and possibly a region of potential instability. The amount of potential instability (if any) **can not** be determined from the imagery, but the imagery can be used to focus on the most likely area for potential instability and on the part of this area where it is most likely to be released.

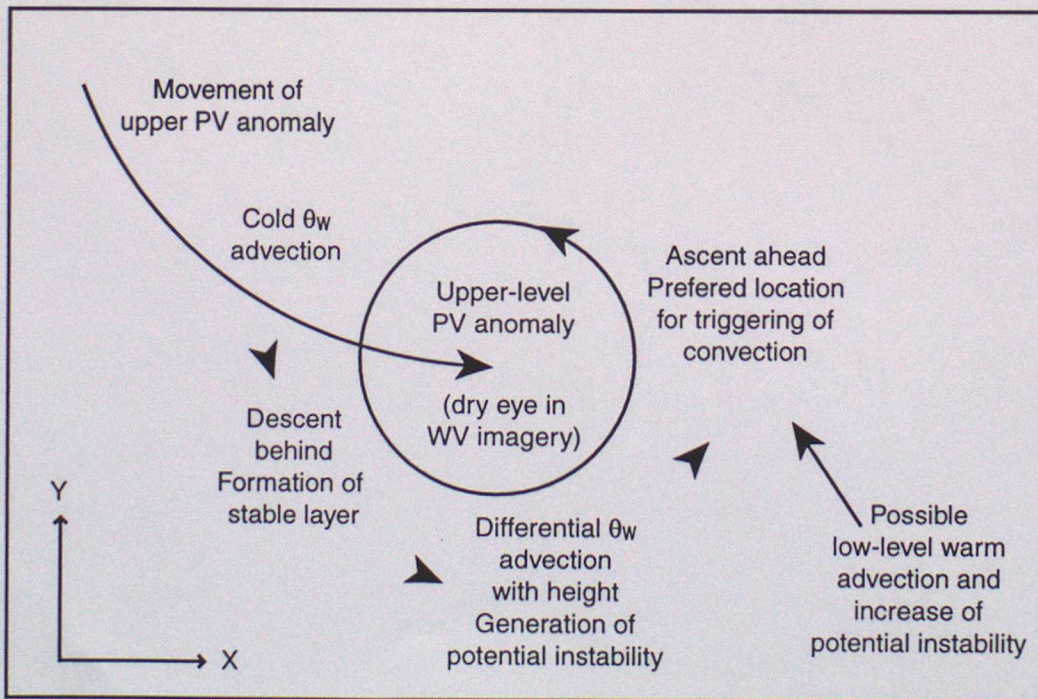
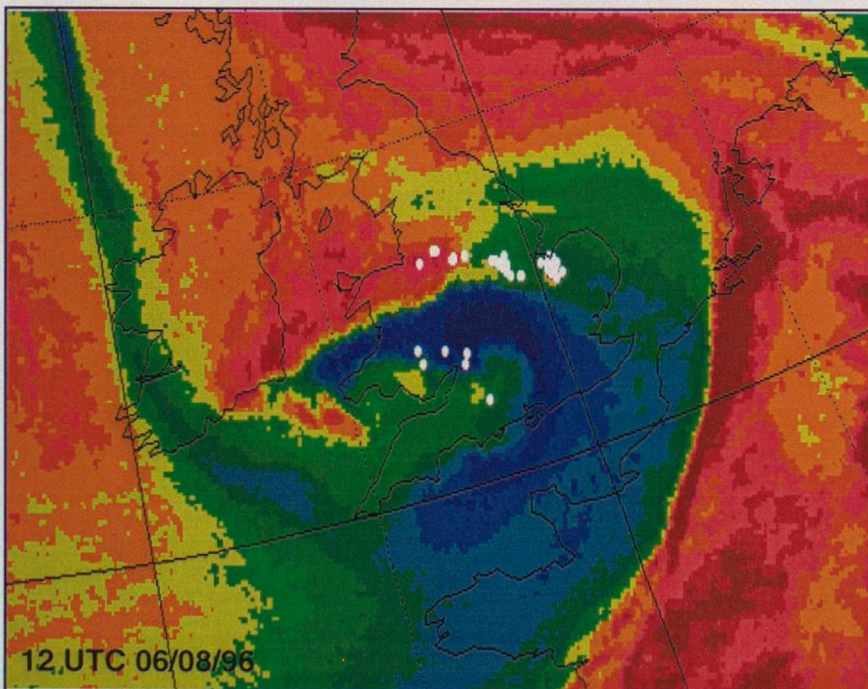
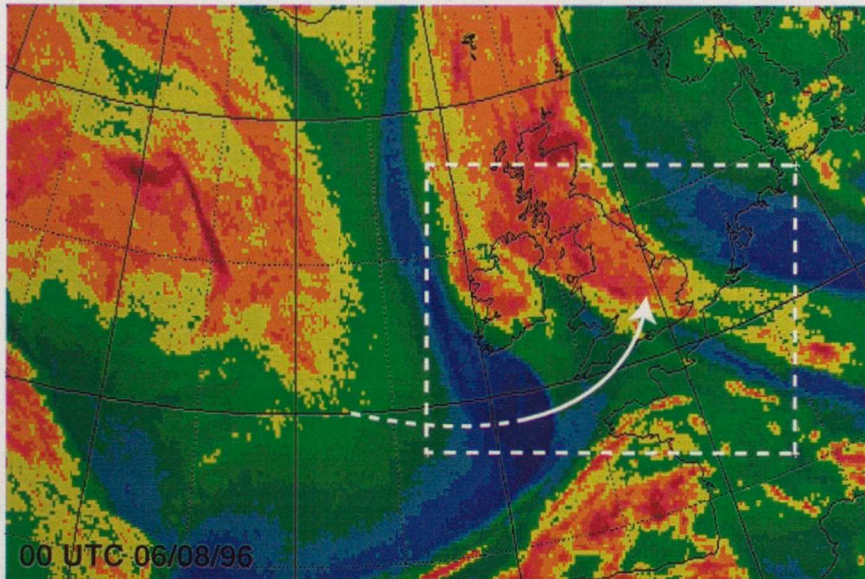


Figure 3. A simple schematic diagram showing the various processes involved in the triggering of convection ahead of a dry eye in WV imagery (isolated upper-level high PV anomaly) and they occur relative to the dry eye. The exact geometry of the situation varies from event to event.

2.2 Dry edge thunderstorms

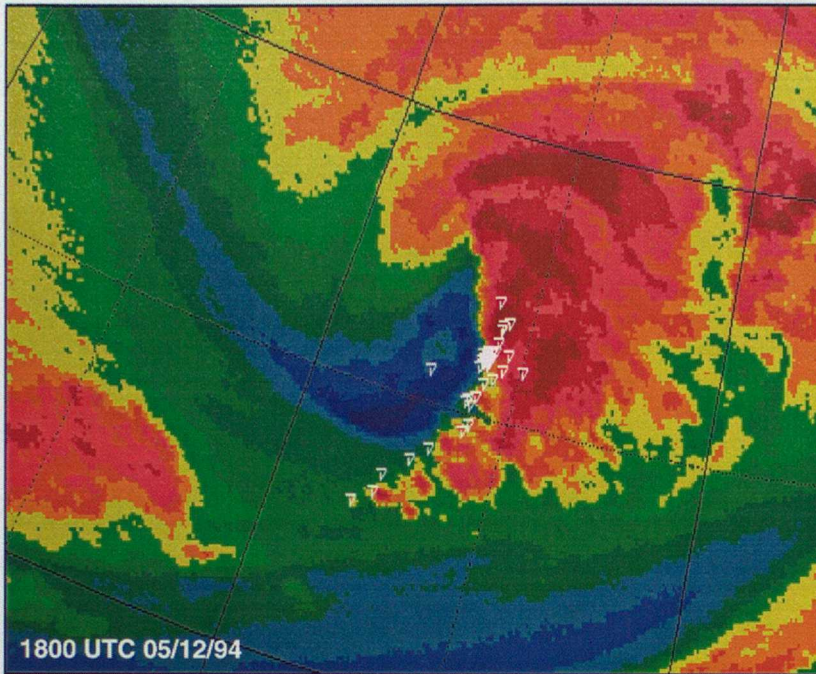
The mechanisms responsible for the development of 'dry edge' thunderstorms are actually the same as for dry eye thunderstorms. The main differences are to do with the greater baroclinicity and scale usually associated with dry edge events. Dry edge thunderstorms occur on the forward edge of dry intrusions in WV imagery. They can be severe and on some occasions lead to intense squall lines. Similarities and differences between dry edge and dry eye thunderstorms will be discussed after the following examples of dry edge thunderstorms seen in WV imagery.

Dry edge thunderstorms - Example 1



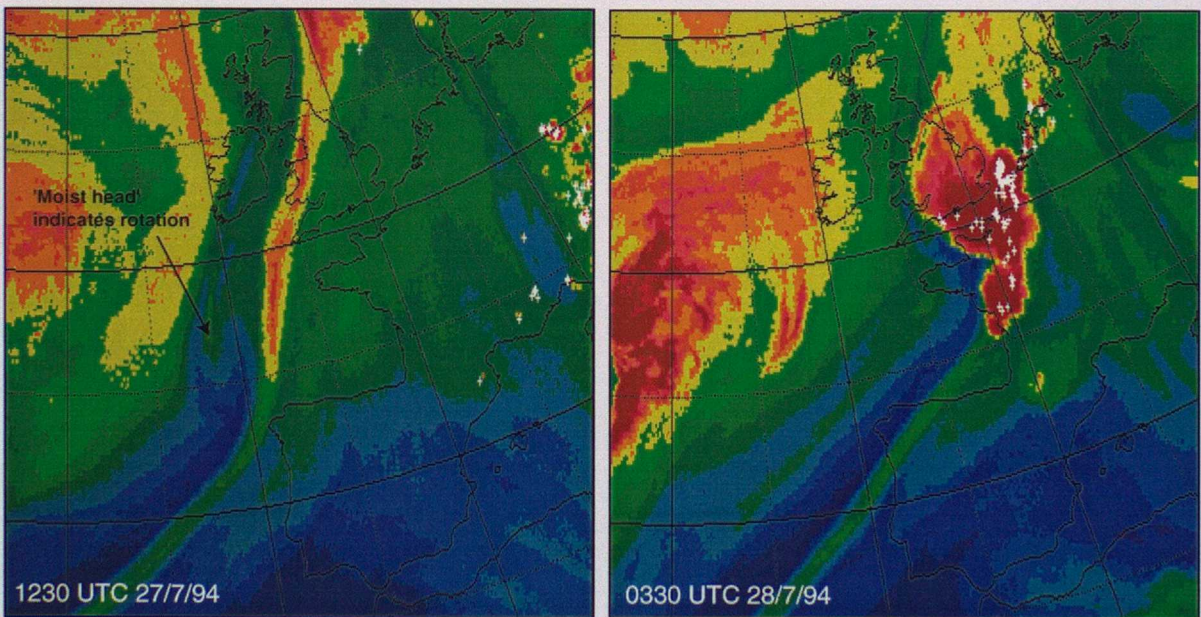
A line of thunderstorms developed over England in the late morning of 6/8/96 on the leading edge of a rotating dry intrusion. Some storms also developed within the dry region itself. White blobs show sferics over a 30-minute interval. Surface cyclogenesis occurred over the UK; these storms were poorly forecast, as were strong gusty winds over southern England behind a surface 'dry line'.

Dry edge thunderstorms - Example 2



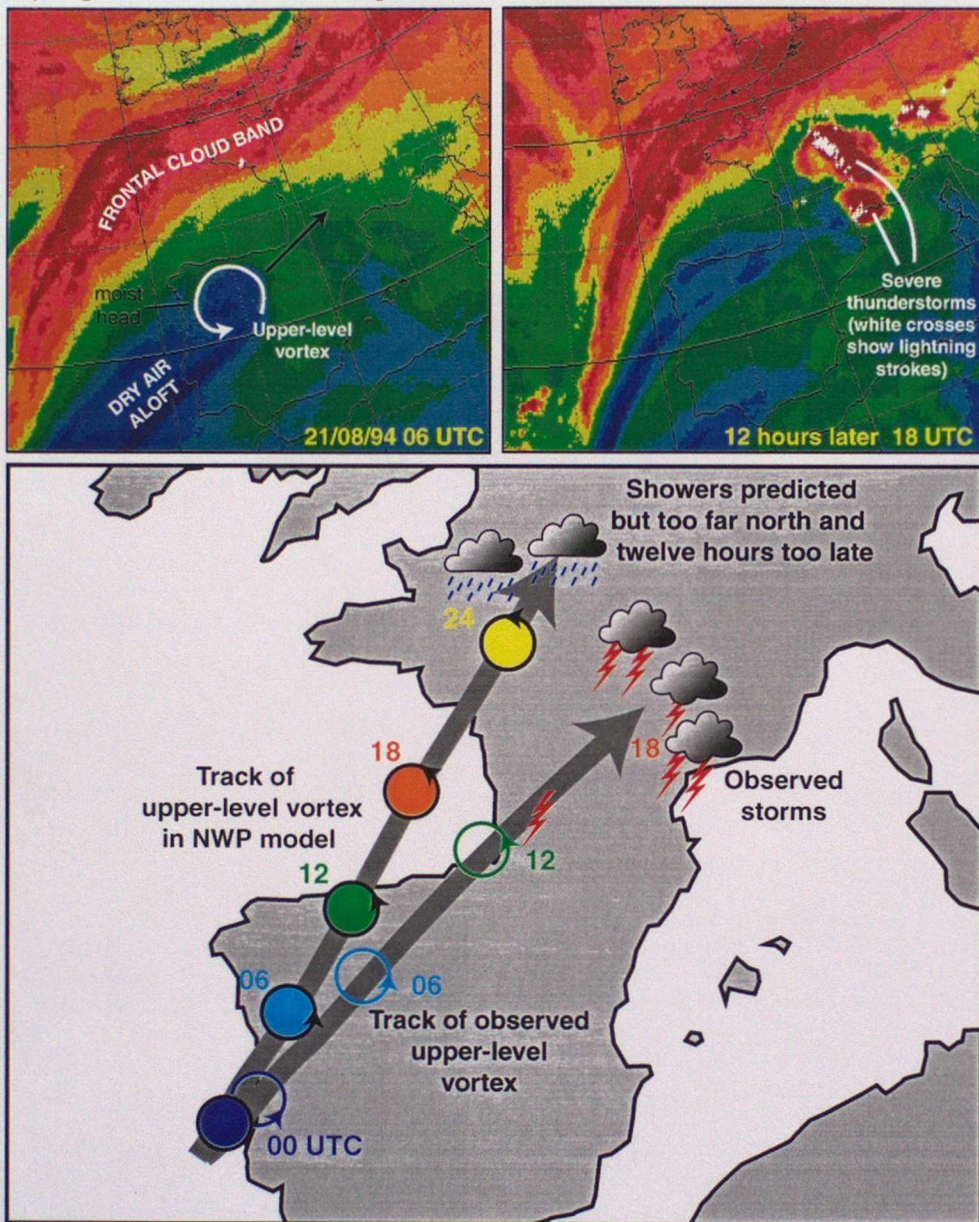
Thunderstorms broke out along the leading edge of a dry intrusion (blue region) on 6/12/94. The white symbols show the sferics (lightning reports) over a 20-minute period. The thunderstorms in this case were intense and associated with a rapid oceanic cyclogenesis event. A brief description of the relationship between the sferics and the dry intrusion is given by Roberts (1995)

Dry edge thunderstorms - Example 3



A mesoscale convective system (MCS) formed on the leading edge of a dry tongue on 27/7/94. The white crosses show sferics over a 40-minute interval. More information can be obtained from a diagnostic study of earlier thunderstorms on the same dry edge (Browning & Roberts (1994)). Upper-level vorticity in the northern part of the dry tongue is evident from the presence of a 'moist head' and the waving moist band ahead of the dry tongue (Again, Browning & Roberts 1994). This MCS was not forecast by the UK Met Office Limited Area Model.

Dry edge thunderstorms - Example 4



A squall line developed on the leading edge of a dry tongue over SW France around midday on 21/08/94. Top panels show WV imagery. White crosses in the top panels show sferics over 40-minute intervals. France and Spain were generally under the influence of an anticyclonic warm plume. The dry tongue showed evidence of rotation from a 'moist head' wrapping around near the northern end. The high upper-level high PV anomaly associated with the dry intrusion could be traced back to much higher latitudes several days before. Thunderstorms were triggered ahead of the upper-level vortex. The bottom panel shows the track of the upper-level vortex diagnosed from the WV imagery (coloured circles) and the track of the 500hPa vorticity anomaly in the operational UK Met Office Limited Area Model run from 00UTC (colour filled circles). It is clear that the two tracks diverge significantly after starting in close proximity and this has a huge impact on the accuracy of the convective rain prediction. Storms that developed over southern France were not predicted at all by the model. The model instead developed convective precipitation the next day over northern France consistent with the location of its own upper-level vortex. Triggering in the model occurred too late and in the wrong place because the predicted upper-level vortex moved over the relatively cool water of the Bay of Biscay instead of over the strongly heated land as it should have.

2.2.1 The large-scale trough pattern

The focus is switched from the smaller scale dry eye features to larger scale troughs and jet regions. As with dry eye events, the transport of low- θ_w air to lower latitudes is essential and occurs, but on a much larger scale. As upper-level troughs extend so the combination of tropopause folding just behind the jet stream bounding the trough and large-scale tropospheric descent can be identified in WV imagery as characteristic crescent shaped dark zones. Mid/upper tropospheric air associated with these dark zones may be advected a considerable distance equatorwards. The picture by Danielsen (1964) shown as Figure 7 of JCMM report 109 is very useful for visualisation of typical air-parcel trajectories. Dark zones at the base and western flank of troughs identify where air parcels that have been advected equatorwards have also experienced the greatest descent (because of being within the baroclinic trough boundary region). The troposphere beneath these dark zones/dry-intrusions is where the greatest likelihood for any potential instability exists, although any potential instability may not be immediately released.

The pattern and evolution of troughs and associated dark zones varies greatly in scale and complexity. It is therefore worthwhile to be able to extract from this complexity a basic framework for the typical trough/ridge evolution associated with dry-edge thunderstorms. This is best done by referring to the two paradigms of baroclinic life cycle behaviour described by Thorncroft et al (1993). Thorncroft et al describe the variation in upper-trough evolution in terms of two extreme scenarios 'anticyclonic' and 'cyclonic' shown by the schematics (a) & (b) in Figure 4. The anticyclonic or LC1 type exhibits strong equatorwards transport during the early cyclonic stage followed by trough stretching and rearward (NE-SW) tilting before a cut-off high PV region is left behind. The cyclonic or LC2 type is characterised by a broad cyclonic wrap-up of the trough with much less meridional extension. As shown in Figure 4 by the thunderstorm symbols the dry edge thunderstorms occur at an earlier stage in the LC2 type than the LC1 type. The LC2 storms occur on the leading edge of the cyclonically turning re-ascending part of the trough. This is where forward sloping (or kata) cold fronts of Browning & Monk (1982) are often observed. Observational studies of overrunning dry air have been supported by Parker (1999) who showed that forward sloping cold fronts can be formed in a two-dimensional semi-geostrophic model of a frontal zone.

The LC1 storms occur on the leading edge of the cut-off at the end of the life cycle. The cut-off may well become somewhat distorted and the WV imagery dark zone take on the appearance of a crescent shape. A cut-off on a small scale is better defined as a dry eye feature. Dry-edge thunderstorms associated with developing cyclones appear to be usually LC2 type whereas dry-edge thunderstorms associated with the breakdown of a hot spell over Europe (especially SW Europe) in summer seem to be mostly LC1 type.

2.2.2 Smaller scale vorticity anomalies

The two above scenarios from Thorncroft et al define the two ends of the spectrum in the large-scale trough pattern. Smaller scale features are frequently superimposed on the large scale and focus the region for thunderstorm development. Convection can be focussed in the vicinity of upper-level vorticity (or PV) anomalies on the edge of a larger scale trough (often at a jet-stream left exit region). Such vorticity anomalies in baroclinic regions are not as easy to observe in WV imagery as in a simple dry eye case; nevertheless they can be identified on many occasions either by playback of animations or by identification of a 'moist head' (Browning & Roberts 1994). The moist head is a tongue of moister air that wraps round and ascends into the dry intrusion region and is a characteristic signature of an upper-level vorticity anomaly. A moist head can be seen in examples 2 & 3.

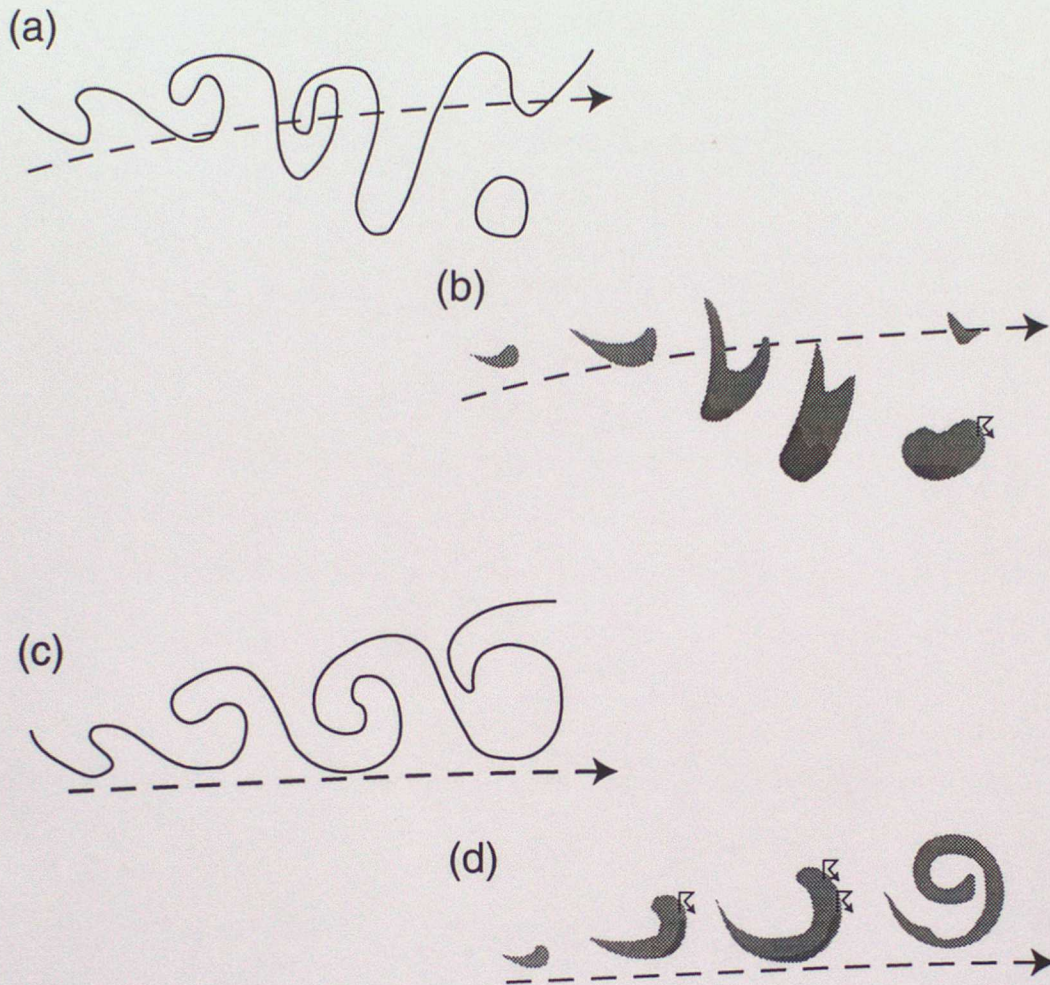
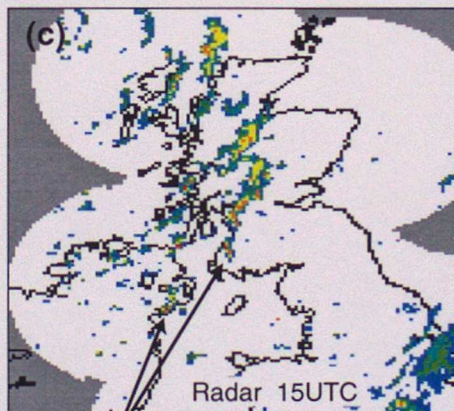
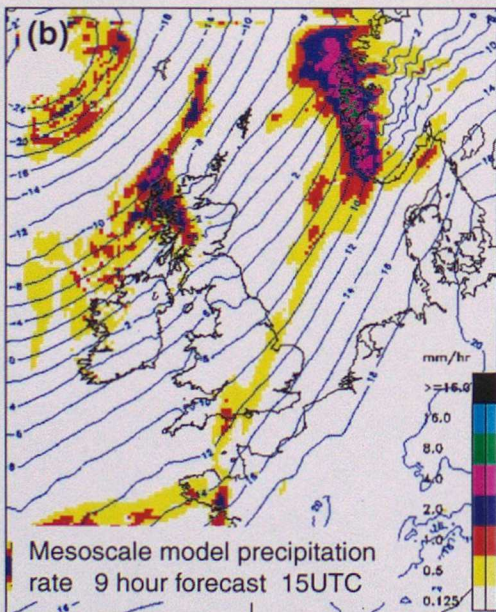
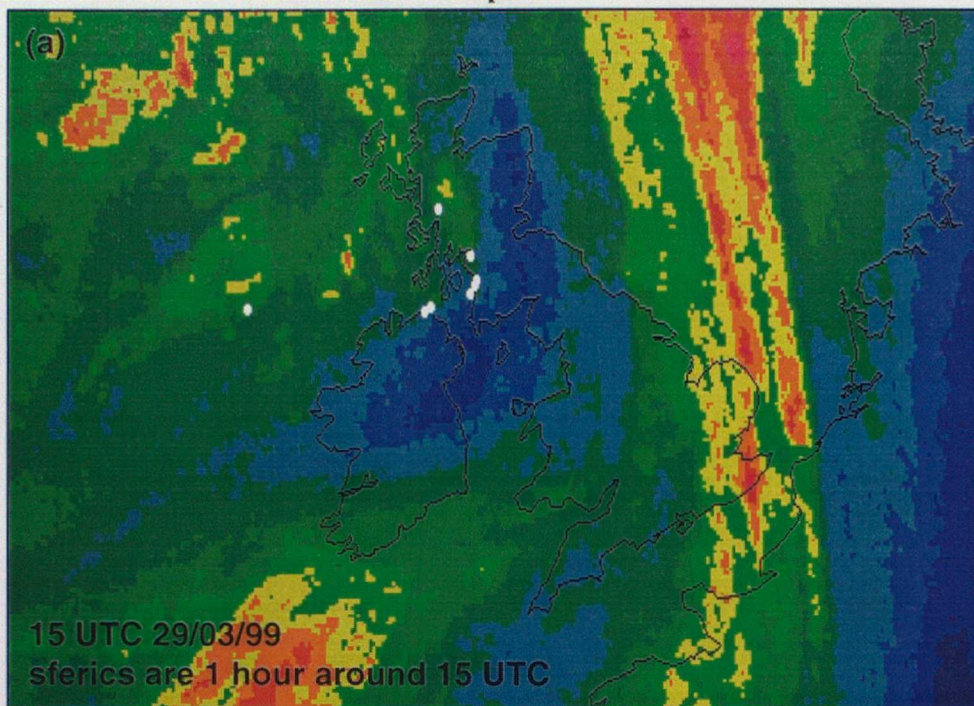


Figure 4. (a) & (c) Schematic of a PV-theta contour in an Atlantic storm track sharing its main characteristics with (a) an LC1 or anticyclonic-type life cycle and (c) an LC2 or cyclonic-type life cycle. The dashed line marks the approximate position of the mean jet at each stage. Taken from Thorncroft et al (1993). (b) & (d) Schematic of the water vapour imagery dark zone signature typically associated with (b) LC1 type and (d) LC2 type. The most likely regions for thunderstorm development are shown by the 'thunderstorm' symbols.

2.3 Inner crescent rim thunderstorms

Inner crescent rim thunderstorms are somewhat different in character to the dry eye and dry edge storms. The thunderstorms occur in the cold air beneath the poleward edge of the jet stream bounding a broad trough (cold trough A in Figure 11 of JCMM report 109) where the WV imagery dark (blue) zone has a gradual transition towards lighter (red/yellow) shades within the trough. Often, though lightning is detected the convective cloud tops do not appear particularly significant in infrared imagery compared to shower clusters in the interior of the trough.

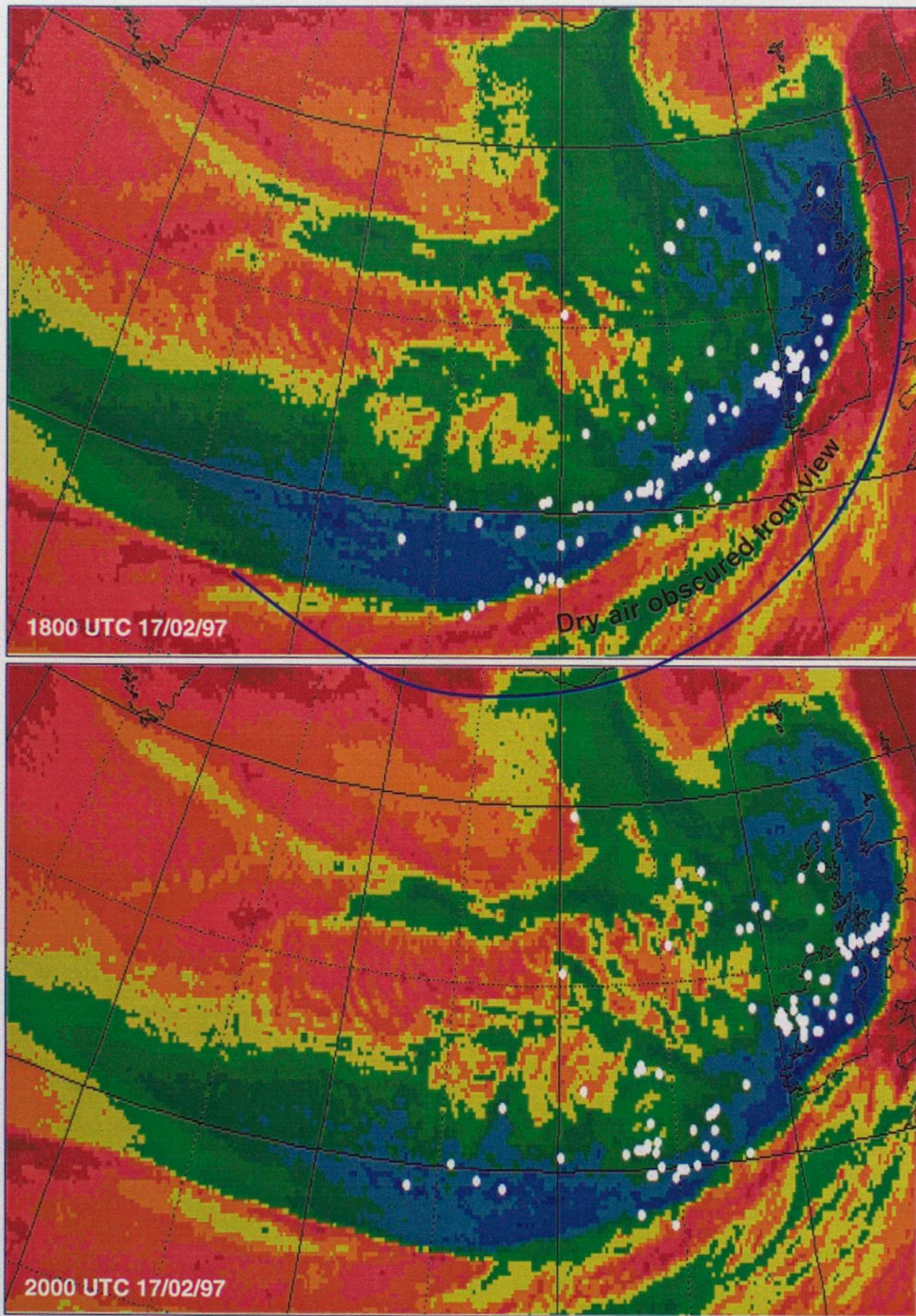
Inner crescent rim thunderstorms - Example 1



Heaviest thundery showers absent in the mesoscale model precipitation field even though the general precipitation forecast is good.

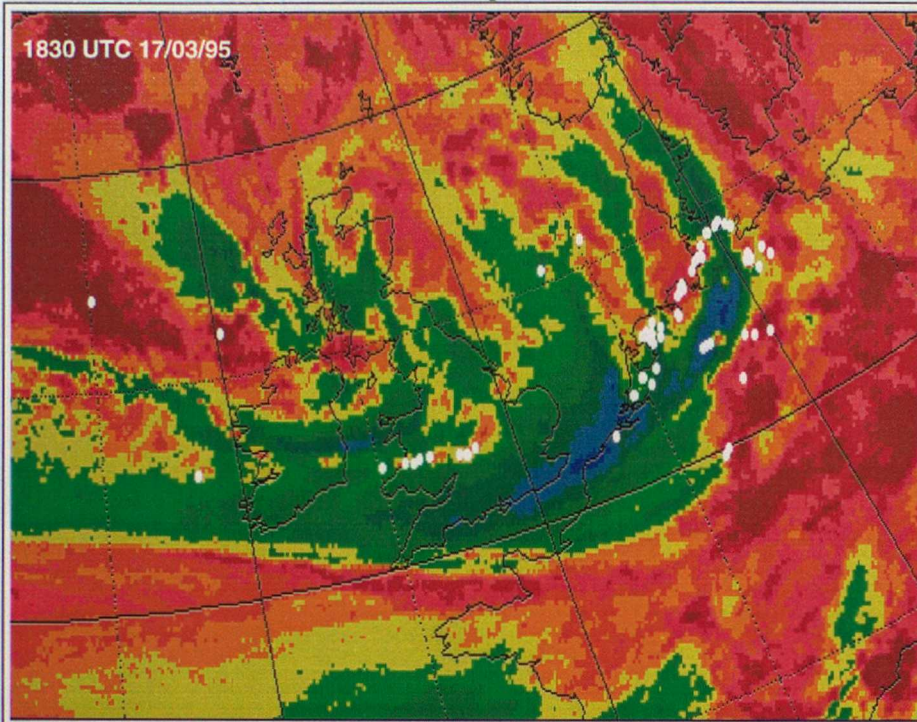
A showery southwesterly flow over Northern Ireland and Scotland on 29/03/99. (a) WV image 15UTC. White blobs show sferics, mostly along the inner rim of the crescent shaped dry intrusion. Notice that, away from the dry intrusion to the northwest of Scotland the orange blobs indicate deeper and larger convective clouds, yet there are no lightning reports. The locally darker blue part of the dry crescent over the Irish Sea and Ireland suggests there may be a small upper-level vorticity anomaly. (b) A 9 hour mesoscale model forecast of precipitation rate (colours) and surface pressure (contours) for 15UTC. (c) UK radar network picture for 15UTC. Although the mesoscale model forecast was good at predicting showers over Western Scotland in this example, the most intense convection over Northern Ireland and Southern Scotland was missed. Reasons for this could be suggested; the dry intrusion may have been misplaced because of a poor analysis, the structure of the stable layer below the inner crescent rim of the dry intrusion may not have been correctly resolved.

Inner crescent rim thunderstorms - Example 2



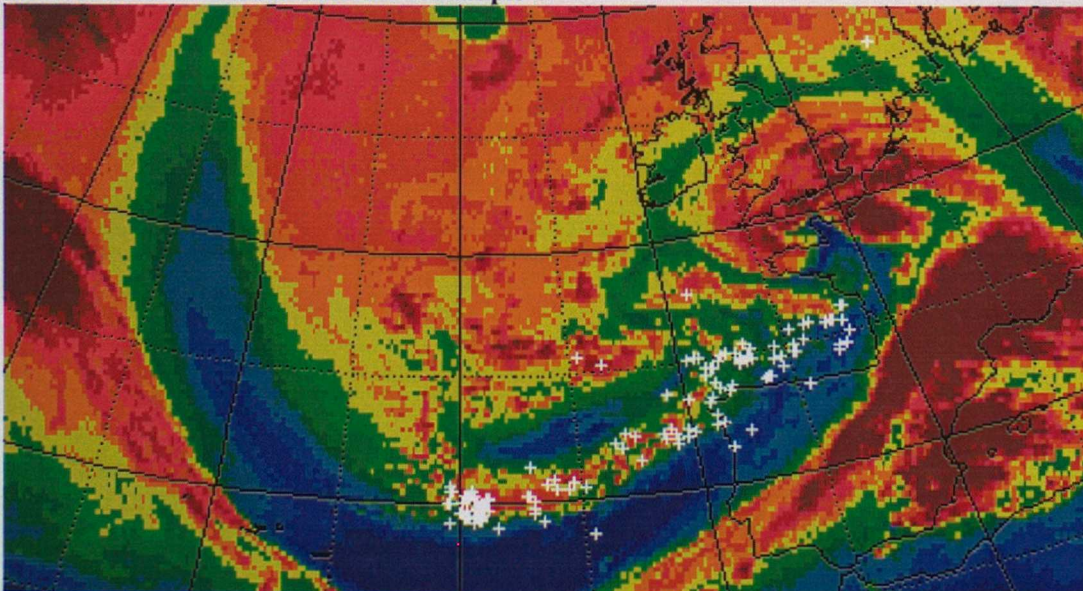
WV imagery from 17/02/97. The white blobs show sferics over an hour centered at the time of the frame. The thunderstorms occurred mostly beneath the blue/dry region in the imagery. In this case the sferics do not appear to be within the inner fringe of the dry intrusion because most of the dry intrusion is obscured from view by high cloud above. The leading edge of the dry intrusion in the lower troposphere is shown by the blue line in the first frame (from mesoscale model - see Figure 9, JCMM report 109).

Inner crescent rim thunderstorms - Example 3



A showery westerly flow over NW Europe on 17/03/95. This was a rather complex looking dry intrusion. The white blobs show sferics over a half-hour period. The thunderstorms were mostly detected along the inner rim of the dry intrusion crescent which was becoming obscured by convective cloud. Thunderstorms were also detected along the leading edge of the dry intrusion. Notice again how few sferics there were over the North Sea, Scotland and Northern Ireland despite the appearance of deeper and larger clouds. Unexpected strong gusts of wind occurred at an earlier time over southern England under the dry intrusion just to the south of the sferics.

Inner crescent rim thunderstorms - Example 4



The large blue dry intrusion marks the base of a large trough over the eastern Atlantic at 0300UTC, 24/10/99. The white crosses mark the sferics, over a 3-hour period, along the northern edge of the dry intrusion.

In the context of the Thorncroft et al LC1 and LC2 trough evolution types, the inner crescent rim thunderstorms occur predominantly along the inner fringe of crescent shaped dry intrusions associated with the broad trough LC2 'cyclonic' type as shown in Figure 5(d).

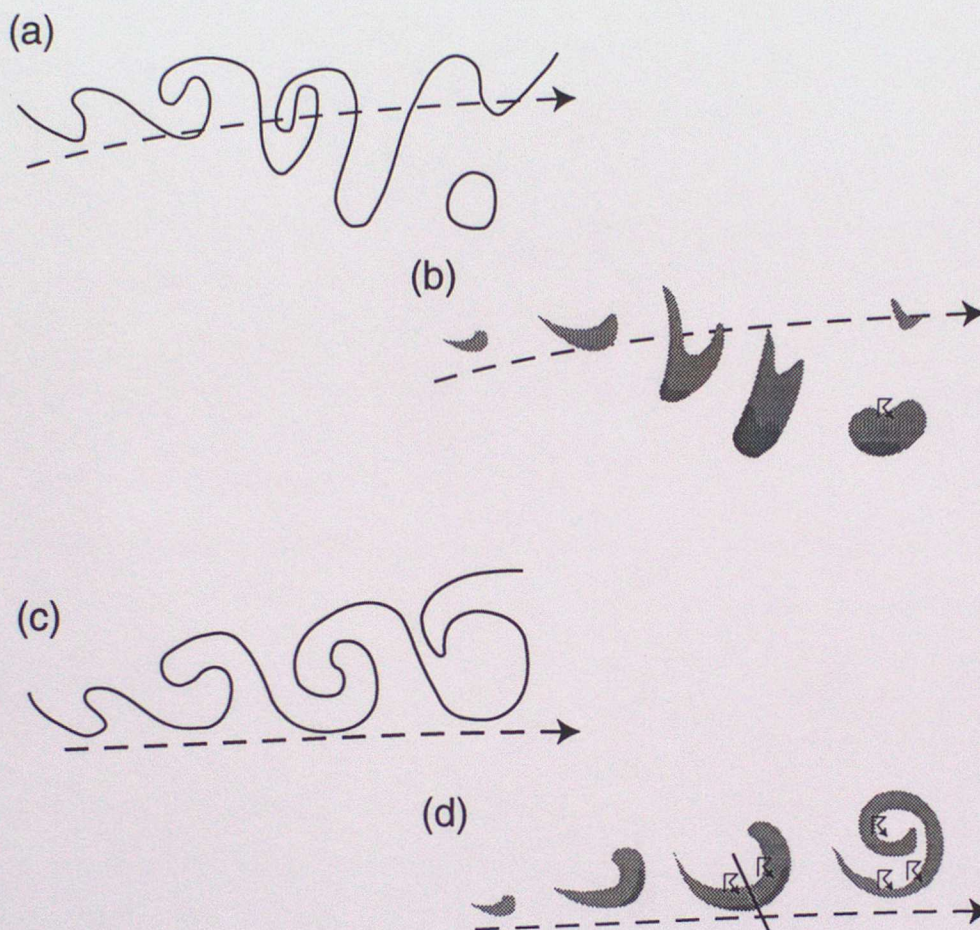


Figure 5. (a) & (c) As for Figure 4. (b) & (d). As for Figure 4 but with the most likely regions for inner crescent rim thunderstorms shown as the 'thunderstorm' symbols. The solid line in (d) represents the rough axis of the schematic cross-section shown in Figure 6.

2.3.1 Why the inner edge of a crescent shaped dry intrusion?

The vertical structure of the atmosphere below a dry intrusion and the horizontal variation in this vertical structure are both crucial in determining where convection will be inhibited and where the most intense convection is most likely to occur. The cross-section in Figure 6 provides a visualization of the typical vertical structure and this cross section will now be used to provide some insight into why inner crescent rim thunderstorms occur where they do.

Refer to Figure 6. Three distinct layers of air can be seen below the jet core.

- (1) The dry intrusion. Air is partly or all of stratospheric origin and is characterised by high potential vorticity, low relative humidity, high potential temperature and high wet-bulb potential temperature.
- (2) Mid-tropospheric air. Air is descending or has recently descended. Wet-bulb potential temperature is low compared to the dry-intrusion air above and may be lower than the boundary-

layer air below. Potential temperature is higher than the boundary layer air below and lower than the air in the dry intrusion. Potential vorticity is low. Relative humidity is usually low but varies.

(3) Boundary layer/lower tropospheric air. The wet-bulb potential temperature may be higher than the layer above. The potential temperature is lower than the air above.

Convection has different characteristics according to where it is triggered and can be split into three distinct regions A, B & C.

A Beneath the southern/middle part of the dry intrusion any convection is capped by the lower stable layer and is therefore shallow. The potential instability through the middle troposphere may be large and hence there is a potential for strong convection but the temperature cap is strong enough to prevent deep convection from occurring.

B The lower stable layer is either weaker because of less slantwise descent than in region A or is reduced because of local slantwise ascent. Convection may be able to break through the lower stable layer and release any mid-level potential instability to produce deep convection and thunderstorms. Deep convection may only occur sporadically where the lower stable layer is still strong. The strength of the convection is dependent on the potential instability and the strength of the stable layer that is overcome and is therefore likely to be greatest towards region A where the inversion is stronger and the boundary layer warmer. Convection may be enhanced in region B ahead of upper level shear generated vorticity anomalies on the northern edge of the jet stream.

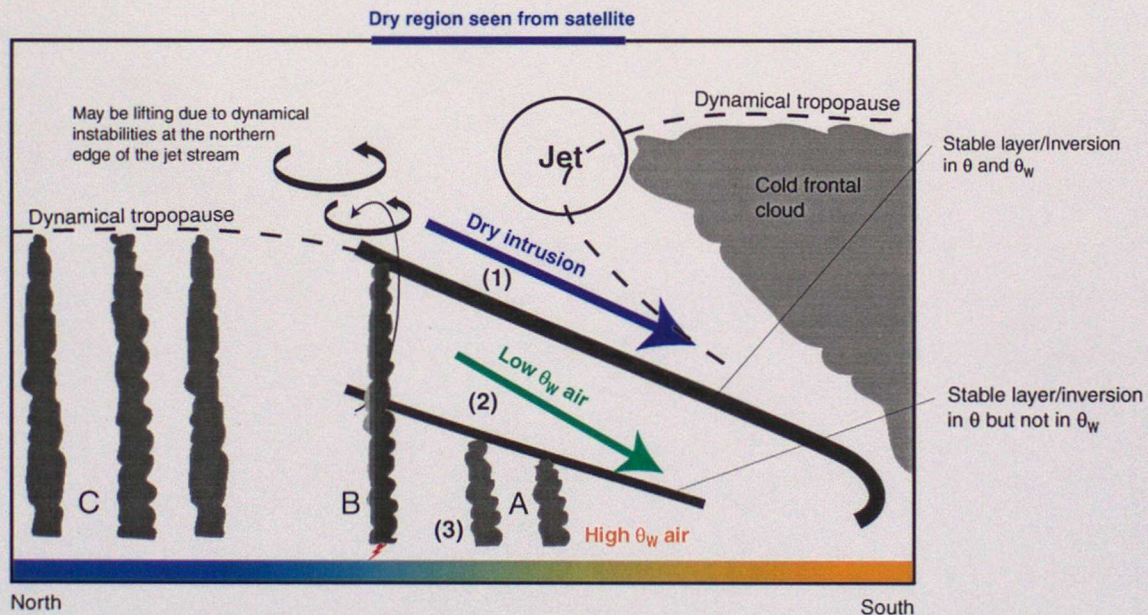


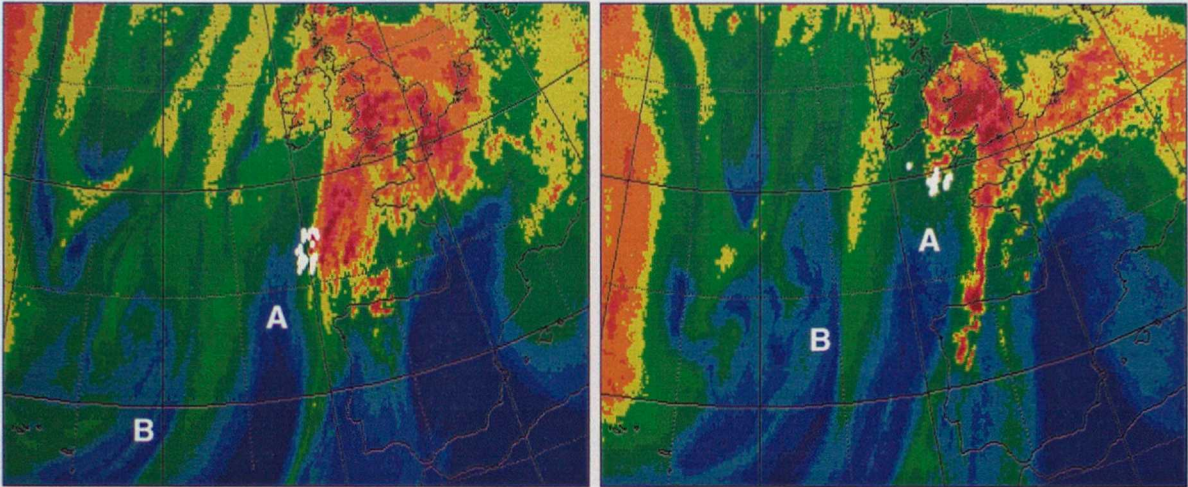
Figure 6. Schematic cross section through a crescent shaped dry intrusion. The solid line in Figure 5(d) gives a schematic indication of the cross-section location. The mesoscale model cross section of relative humidity shown in Figure 9 of JCMM report 109 is complimentary to this figure.

The vertical motion associated with such anomalies can act to reduce the strength of the lower stable layer and lead to organised convective clusters or comma clouds.

C Deep convection can occur more easily than in region B because there is no lower stable layer to break down. However, the convection is not as intense for two reasons; firstly, the lack of a stable layer means that less Convectively Available Potential Energy (CAPE) can be stored before convection occurs; secondly, the boundary layer/lower tropospheric air is likely to be cooler.

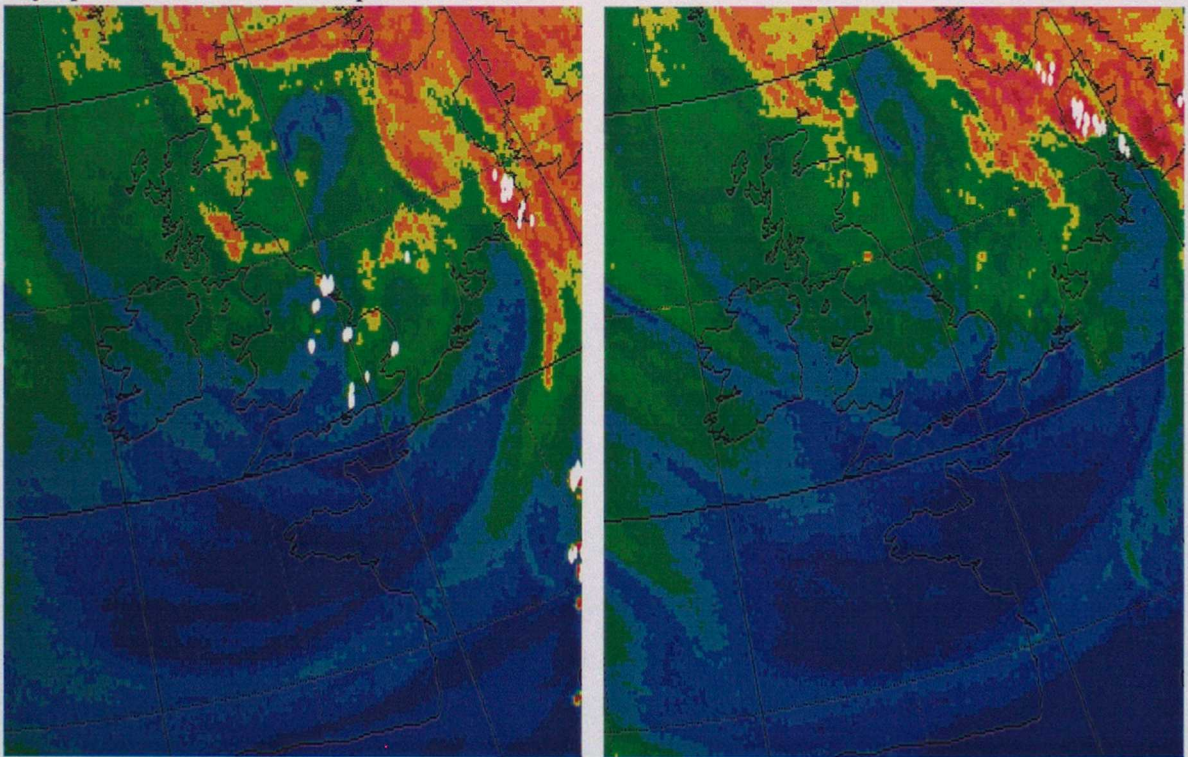
2.4 Dry tip thunderstorms

Dry tip thunderstorms - Example 1



Meteosat water vapour images from 00 & 09 UTC 20/06/98. White crosses show lightning reports over a 30-minute interval. Thunderstorms occur on the northern 'tip' of dry region A. Storms later occur at the tip of dry region B.

Dry tip thunderstorms - Example 2



Meteosat water vapour images from 18 & 21 UTC 27/06/98. White crosses show lightning reports over a 30 minute interval. Thunderstorms over Denmark developed on the NE tip of the dry intrusion.

2.4.1 Why the 'dry tip' category?

Dry tip thunderstorms share many similarities with the other types mentioned so far, as well as some differences.

The basic mechanism for thunderstorm development at a 'dry tip' is the same as for the other types in that potential instability, initially prevented from premature release, is eventually released by local or synoptic scale ascent. The potential instability occurs primarily as a result of the transport of cold air at middle levels from higher to lower latitudes in association with WV-imagery dry intrusions.

The difference can be revealed in terms of the synoptic scale pattern. Dry tip thunderstorms occur on the forward, poleward tip of dry intrusions that have become stretched and elongated. The stretching could be of an LC1 anticyclonic type filament or of a dry crescent associated with an LC2 cyclonic type. In the case of the LC1 type, a dry tip in WV imagery can be indicative of a vorticity anomaly at the end of an upper-level PV filament or of a low-level vorticity anomaly beneath an upper-level PV filament. Either one of these scenarios is associated with some slantwise ascent that could lead to convective triggering. In the case of the LC2 type, large-scale slantwise ascent occurs along the forward part of the trough where air is transported poleward (see Figure 5(c)) and can result in convective triggering. The difference between this and the dry edge situation is that the triggering is more often associated with large-scale ascent in a quasi-stationary pattern rather than ascent associated with a distortion of the flow and significant overrunning. Interestingly, deep convection is sometimes observed at the end of cloud bands aligned along the dry intrusion (along the thermal wind) and hence triggered earlier than expected (Browning & Roberts 1995). There is still uncertainty as to whether such cloud bands may be the result of a local instability such as Conditional Symmetric Instability (CSI).

2.5 Warm plume thunderstorms

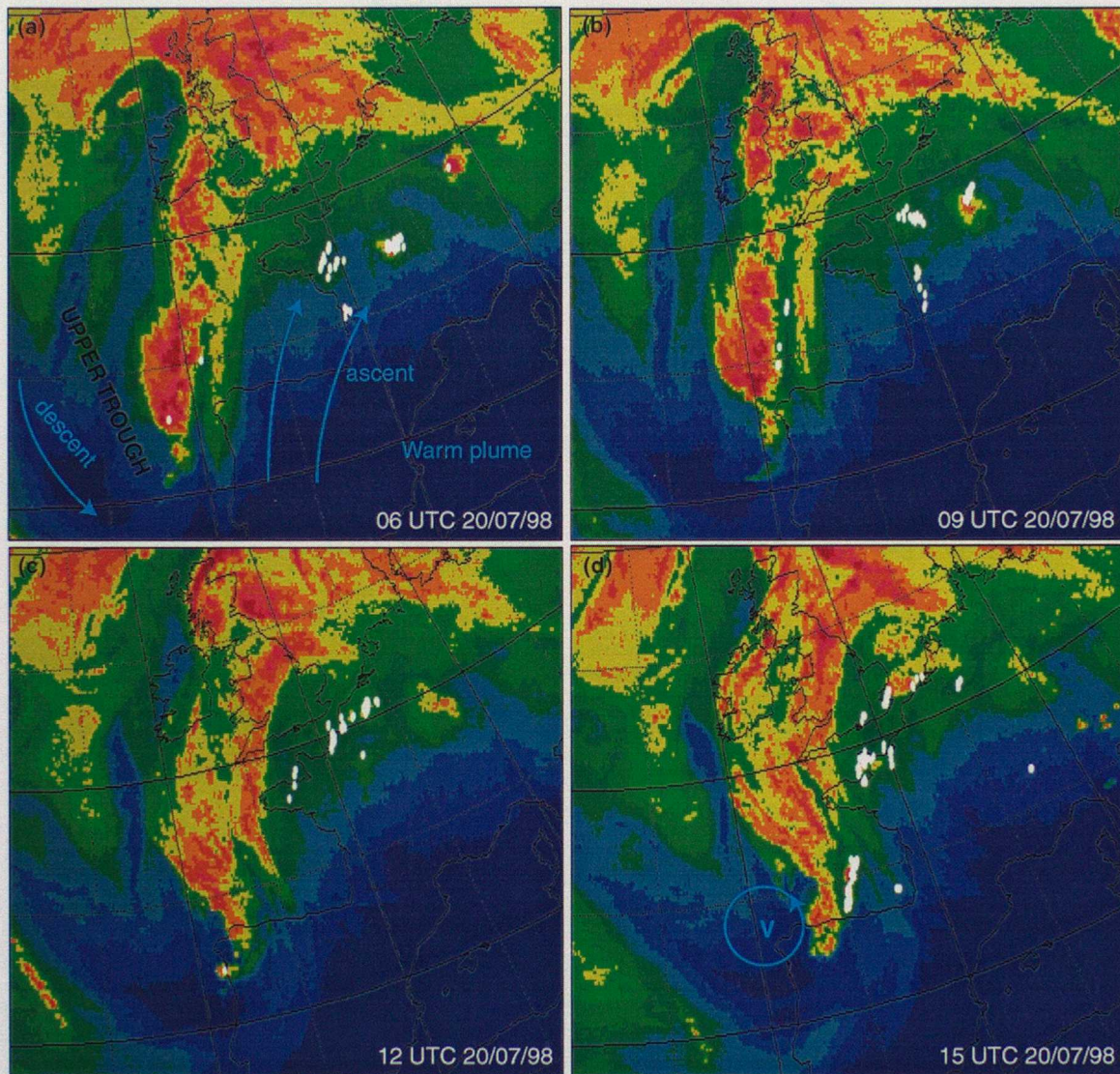
This category stands alone because it has nothing to do with the previous examples of WV imagery blue (dark) zones that indicate a lower tropopause and transport of lower θ_w air from higher latitudes. Potential instability is not generated through differential advection.

A warm plume is also identified in WV imagery as a blue (dark) region, but the warm brightness temperatures are a consequence of warm, dry upper-tropospheric air below a high tropopause. Warm plumes are located within upper-level ridges (see Figure 11 in JCMM report 109). The air is warm and dry, either as a result of sub-tropical descent or because the air originated over a strongly heated dry surface such as the Sahara or Spain in summer. The vertical temperature profile of these warm plumes can be nearly dry adiabatic over some depth. On some occasions warm-plume air is advected northwards ahead of an upper-level trough and air parcels gradually ascend along sloping isentropic surfaces. The WV imagery example from 20/07/98 reveals this ascent and increasing relative humidity as a gradual transition from blue through to green along the direction of the flow. If there is sufficient ascent to produce local saturation then middle-level convection (observed as castellanus clouds) can develop in such an unstable environment (Ludlam 1980). Sometimes scattered thunderstorms break out as shown in the example.

WV imagery is evidently a useful tool for observing warm plumes and regions of ascent, but its usefulness in highlighting a focus region for convective triggering in this category may be limited because of the broad, large-scale nature of warm plumes.

If the leading edge of a dry intrusion associated with the southern flank of an upper-level trough moves into a warm plume region (especially if castellanus storms have already formed) then very intense and long-lived thunderstorms can develop. Such situations produce the most severe storms over Western Europe. In the example, the storms ahead of the upper-level vorticity anomaly over Biscay in (d) later developed into an intense mesoscale convective system.

Warm plume thunderstorms - Example

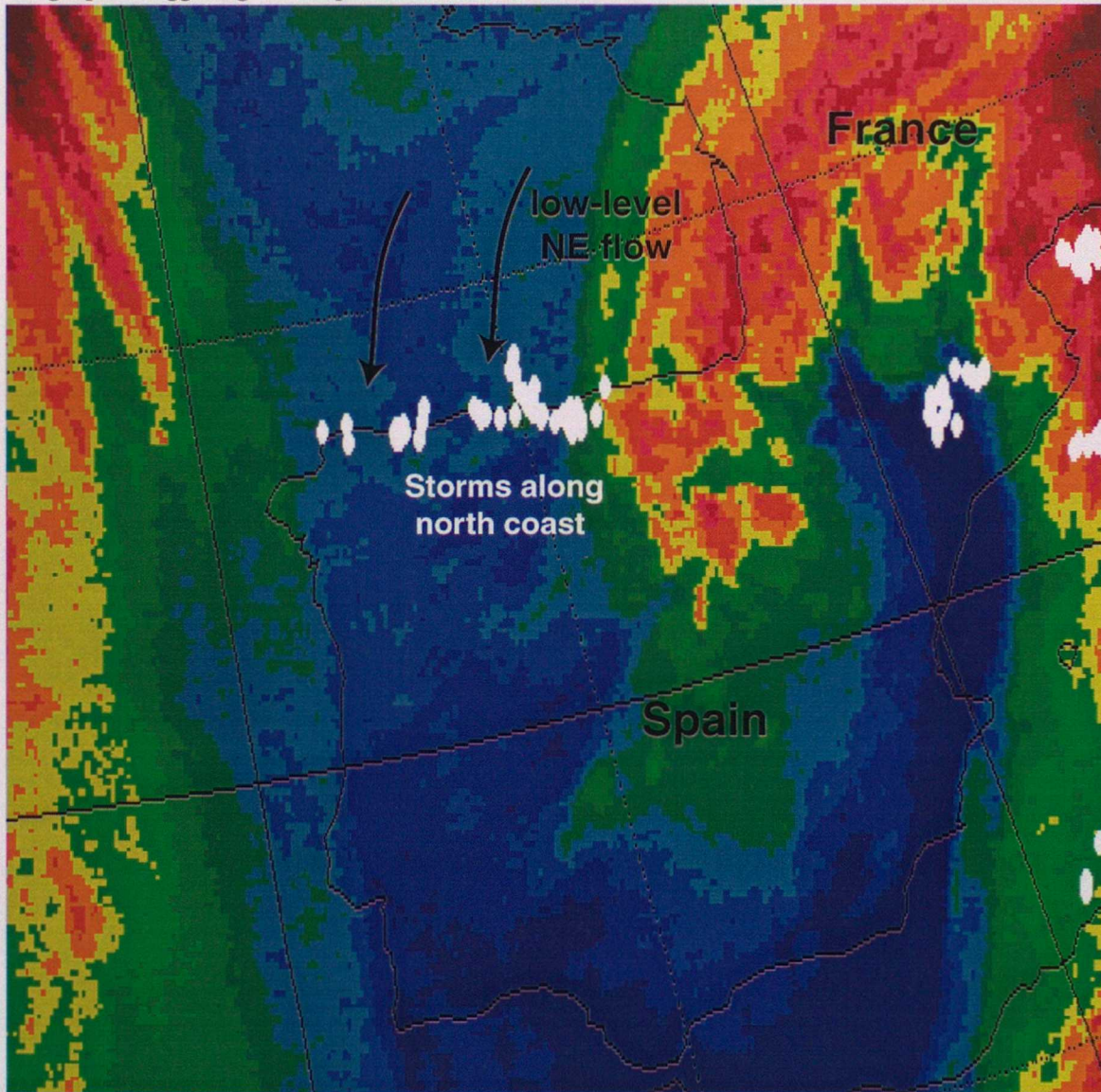


Meteosat WV images for 06-15 UTC 20/07/98 showing thunderstorms on the northern fringe of a warm plume (usual colour scheme). Sferics over 40-minute intervals are shown by white crosses. The warm plume and upper level trough are identified on (a). Light blue arrows show regions of ascent and descent. An upper-level vorticity anomaly is highlighted on (d) by a light blue circle and arrow labelled with the letter V.

2.6 Orographic triggering at a coastal mountain barrier

Heavy showers and thunderstorms can be triggered beneath dry intrusions when uplift due to the flow encountering a mountain barrier is sufficient to release any potential instability. The north coast of Spain (see example below), the west coast of Norway, the west coast of Scotland and Corsica are the best areas for observing this effect.

Orographic triggering - Example



WV image at 06UTC 10/01/99 (usual colour scheme). White blobs show sferics over a 3-hour interval. Thunderstorms occurred along the north coast of Spain beneath a dry intrusion - and at the tip of the dry intrusion over NW Spain.

2.7 A Summary

This section has shown by use of examples, how specific regions associated with patterns in WV imagery can indicate where the likelihood of thunderstorm development is significantly increased.

A summary picture of the typical spatial distribution of lightning risk associated with a typical broad crescent shaped dry intrusion is shown below in Figure 7. The higher lightning risk areas are predominantly found within ascent regions located at the perimeter edges of dry intrusions (whatever the shape of the dry intrusion). A note of caution - any single dry intrusion may or may not be associated with thunderstorms; other factors (e.g. potential instability, surface heating, warm advection) also come into play and a dry intrusion signature should not be used in isolation.

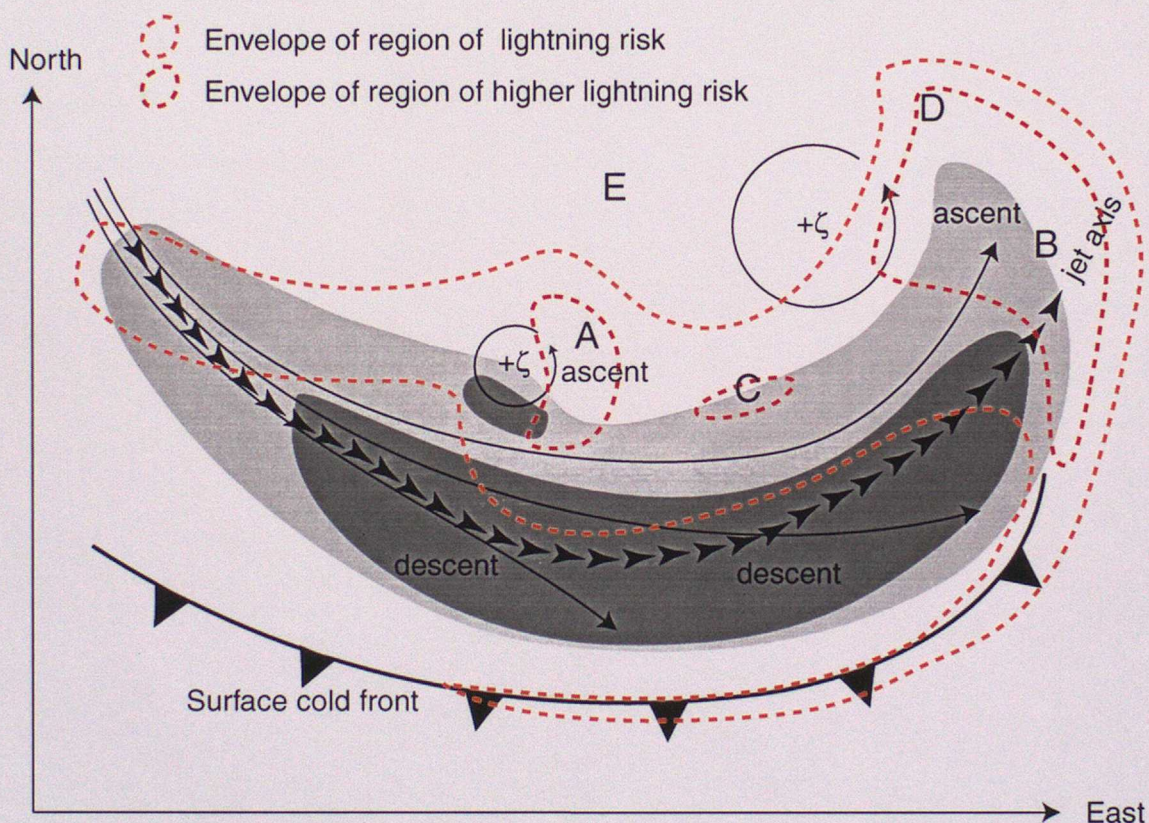


Figure 7. Schematic of a typical crescent shaped dry intrusion seen in WV imagery. The grey shading shows the upper-tropospheric dry region with the driest in the darker shade. Orange and red dashed lines enclose regions of increased lightning risk. Upper-level vorticity anomalies are depicted by the broken circles with arrows. The letters A, B, C & D correspond to the favoured regions for thunderstorm development that have been highlighted by the examples in this section. A - ahead of a small-scale upper-level vortex (a dry eye); B - at the leading dry edge; C - along the inner crescent rim; D - dry tip convection. E shows the area where open cellular convection is common and precipitation may be heavy, but thunderstorms are less likely.

3. A study of the relationship between water vapour imagery and thunderstorms

The previous section has shown several good examples of the relationship between thunderstorm initiation and dry regions seen in WV imagery. Such case studies are extremely valuable and lead to a better understanding of the mechanisms involved in the triggering of some thunderstorms. However, it is important to know how representative this handful of cases really is. The next step is to discover whether the imagery-thunderstorm relationship can be regularly observed or is just restricted to the examples that have been shown. To this end, a study has been performed to discover what proportion of thunderstorms, observed over a fixed area and reasonably long time period, appear to be dynamically linked to dry regions in WV imagery. Details of the approach used and then results are presented below.

3.1 The study

The investigation took place over two time periods - one in the summer and one in the autumn

Summer period	20/06/98	to	16/08/98	(58 days)
Autumn period	23/10/98	to	12/12/98	(51 days)

The area used for the study is defined in Figure 8. This area was chosen to include as much of Western Europe and the North Atlantic as was possible given the limitations of the maximum display area allowed with the PC display program DISP (see acknowledgements). North Africa and Canada are excluded.

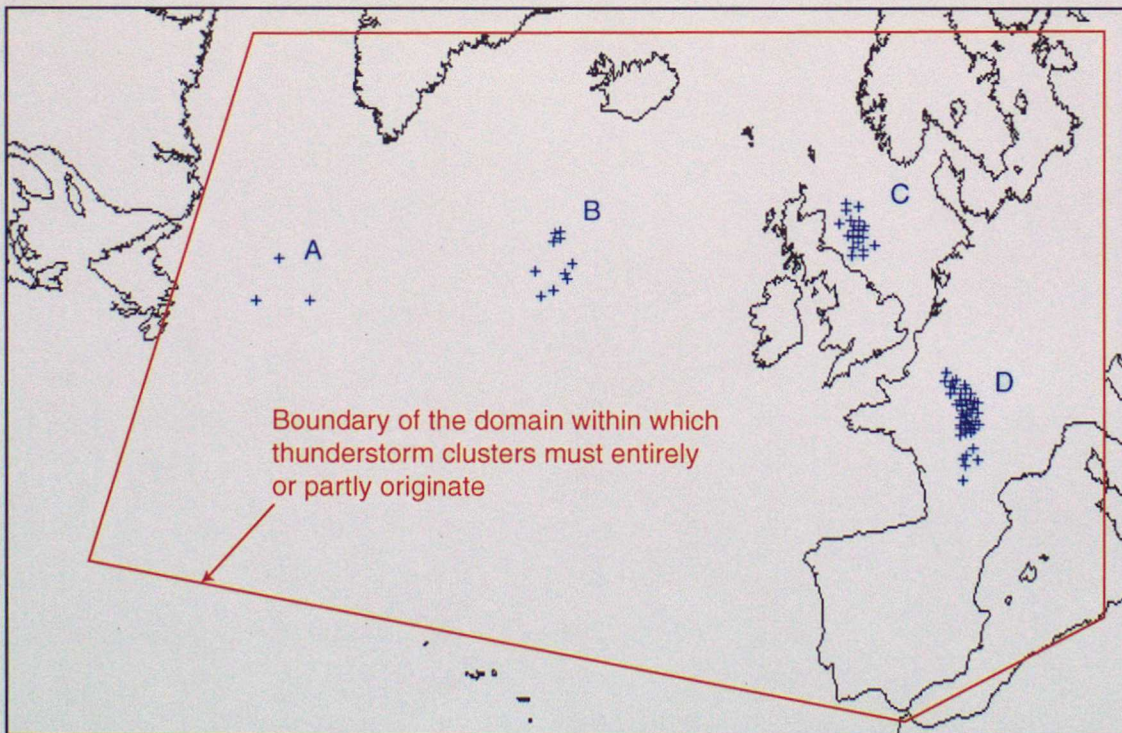


Figure 8. The domain used for the WV imagery and thunderstorms study is defined by the red outline. The significance of the blue crosses and the letters A, B, C & D is explained in the text.

Figure 8. The domain used for the WV imagery and thunderstorms study is defined by the red outline. The significance of the blue crosses and the letters A, B, C & D is explained in the text.

Thunderstorms were identified from sferics detected by the Met Office ATD lightning detection system (Lee 1989). No other method was used to identify thunderstorms. The lightning detection system provides the best and only realistic way of observing the spatial distribution of storms.

The approach used was to identify thunderstorm clusters rather than individual storms. There are several reasons for this. Firstly, it can often be difficult to separate individual storms on the basis of just lightning reports. Secondly, the primary interest here is in the more severe end of the thunderstorm spectrum, so the small, isolated and transient storms were not counted. Thirdly, the ATD system is not sensitive to every single lightning strike so it was not sensible to include the smallest storms as part of the study because an equal number of those small storms may be missed.

A cluster was defined as 8 or more sferics over a 3-hour time window where the maximum separation was no more than 200km and the separation between sferics in a cluster was much smaller than the distance to the next cluster. The criterion reduced to 5 or more sferics if the cluster persisted for longer than a single 3-hour time window. Cluster A in Figure 8 would not have counted; clusters B, C and D would. Once a cluster had been identified, the number of sferics in that cluster was allowed to drop to a single report over a 3-hour time window if there was continuity over several time windows. The clusters must have entirely or partly originated within the boundary of the defined domain to be counted.

Once a cluster had been identified, WV imagery was examined at 3-hourly intervals to see if a relationship existed between the sferics and dry regions in the imagery. The clusters were classified under five headings according to a subjective interpretation of their fit to the imagery.

- | | |
|---------------------|--|
| 1. Very good | A classic case. Extremely obvious relationship with a WV image dark zone |
| 2. Good | Obvious that there is a relationship with the WV imagery |
| 3. Yes | Clear that a relationship exists, but does require more interpretation skills. |
| 4. Possible | Not a clear relationship, but indications that it can't be completely ruled out. |
| 5. No | No relationship with the WV imagery |

The intensity of the thunderstorm clusters were classified according to whether they were severe, medium or weak. Again, there is a subjective nature to this classification. The intensity was primarily determined from the density of the sferics and the dimensions of the most dense area over 3-hourly time periods.

A cluster was defined as severe when sferics, (examples displayed as crosses on the standard full area in Figure 8), merged together with no gaps, and the extent of this dense area was greater than 200km in some direction (e.g. cluster D in Figure 8). A dimension of less than 200km was still sufficient to register a severe storm cluster if either the cluster was very slow moving or the cluster persisted in a dense sferics state for at least three 3-hour time windows. A cluster was defined as weak if the sferics were well scattered and each concentration of sferics was fewer than 10 reports (e.g. cluster C in Figure 8). Medium intensity clusters lay between the two other extremes (e.g. cluster B in Figure 8). This judgement by eye of the severity is obviously going to be flawed and some clusters will have been wrongly categorised, but over a large number of events it gave a good enough indication.

If a cluster was found to have a 'very good', 'good', 'yes' or 'possible' relationship with the WV imagery it was classified according to the type of relationship i.e. 'dry eye', 'dry edge', 'dry tip', 'crescent inner rim' or 'orographic'. Any new cluster that formed on the same part of a dry zone as an existing cluster was classified as the same cluster (unless it was a considerable distance away) because both clusters were associated with the same dynamical forcing. If this approach was not taken, there could be occasions when several thunderstorm clusters triggered on a single dry edge would all be counted and the results would become biased in favour of the WV imagery relationship. As it stands, the method described here is biased in the other sense in that multiple storms related to WV imagery were only counted once.

The duration of each cluster was measured to the nearest 3 hours, along with a note of whether the cluster lasted beyond midnight and originated over land or sea. Problems arose if a cluster moved out of the maximum DISP area. In such a situation, 3 hours were added to the lifetime of an active cluster, nothing was added to a weakening cluster. This is not entirely satisfactory, but over a large number of events where only a small percentage do move out of the area, it probably does not damage the validity of the results too much.

3.1.1 Possible criticism of the method

1. It could be argued that the results are biased because of the subjective nature of the WV imagery interpretation.

This is a fair point, but until an automatic technique can accurately do the job, it is the only way. The examples in the previous section should suggest that for many thunderstorm events the relationship with WV imagery is easy to see. Obviously, the relationship can be more tenuous, but even if some events are classed as having a relationship when they shouldn't, there are other occasions when the opposite is true and thunderstorms associated with dry intrusions are not classified as such because the dry air is obscured from view.

2. The approach of first identifying thunderstorms and then looking for a relationship with WV imagery does not provide information about the number and proportion of dry regions that are involved in thunderstorm development.

It is true, that even if most thunderstorm clusters are triggered in association with WV dry regions, it still may be that only a small proportion of all dry intrusions are involved. If this is the case then the benefit to subjective forecasting may be limited. The problem with identifying the dry regions before the thunderstorms is that individual dry intrusions can persist as separate entities in the imagery for several days and travel hundreds or even thousands of kilometres. In order to do such a study a much larger domain than is possible with DISP is required; then dry regions can be tracked over these large distances. It should be done.

3.2 Results from the summer study (Figures 9, 10 & 11)

Number of days with data	57	
Number of clusters	196	(3.4 clusters per day)

A breakdown of the number of clusters that had a 'good/very good', 'yes' or no relationship with dry features in WV imagery is shown in Figure 9. The 'possible' category has not been included in the bar chart because it does not add much insight. The 'no' category has the largest number of clusters (65), but is significantly less than the 'yes' and 'good' categories combined (89, (53+36)). Figure 9 also displays the number of days when at least one 'yes' or 'good' cluster occurred in

The key results from Figure 9

- 58% of storm clusters (excluding 'possibles' from the statistics) showed a relationship with WV imagery
- 74% of days had a storm cluster related to WV imagery in the domain
- 33% of the storm clusters do not have a relationship with WV imagery

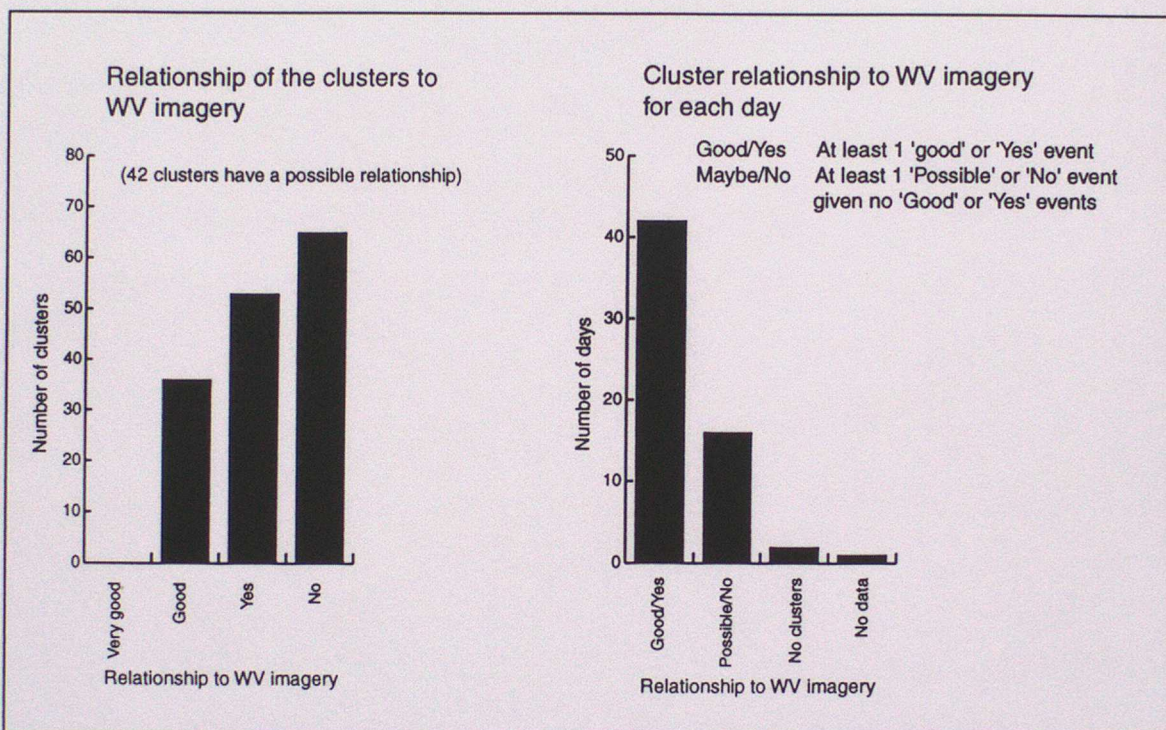


Figure 9.

3.2.1 Summer period, storm cluster duration (Figure 10)

Intuitively, it would seem likely that thunderstorms triggered as a result of upper-level dynamical forcing revealed by a relationship with WV imagery would persist longer than storms triggered by more local conditions. This has been investigated.

The duration of storm clusters has been grouped into 6-hour bins and is shown in Figure 10(a). The smallest duration categorised is 3-6 hours (rather than 0-6 hours); this is because the information was gathered at discrete 3-hourly intervals and anything less than 3 hours is beyond the accuracy of this experiment.

As might be expected, the peak is at the shortest duration of 3 to 6 hours and tails away towards the longer time periods. A significant proportion, around 30% of the storm clusters, persist for longer than 12 hours.

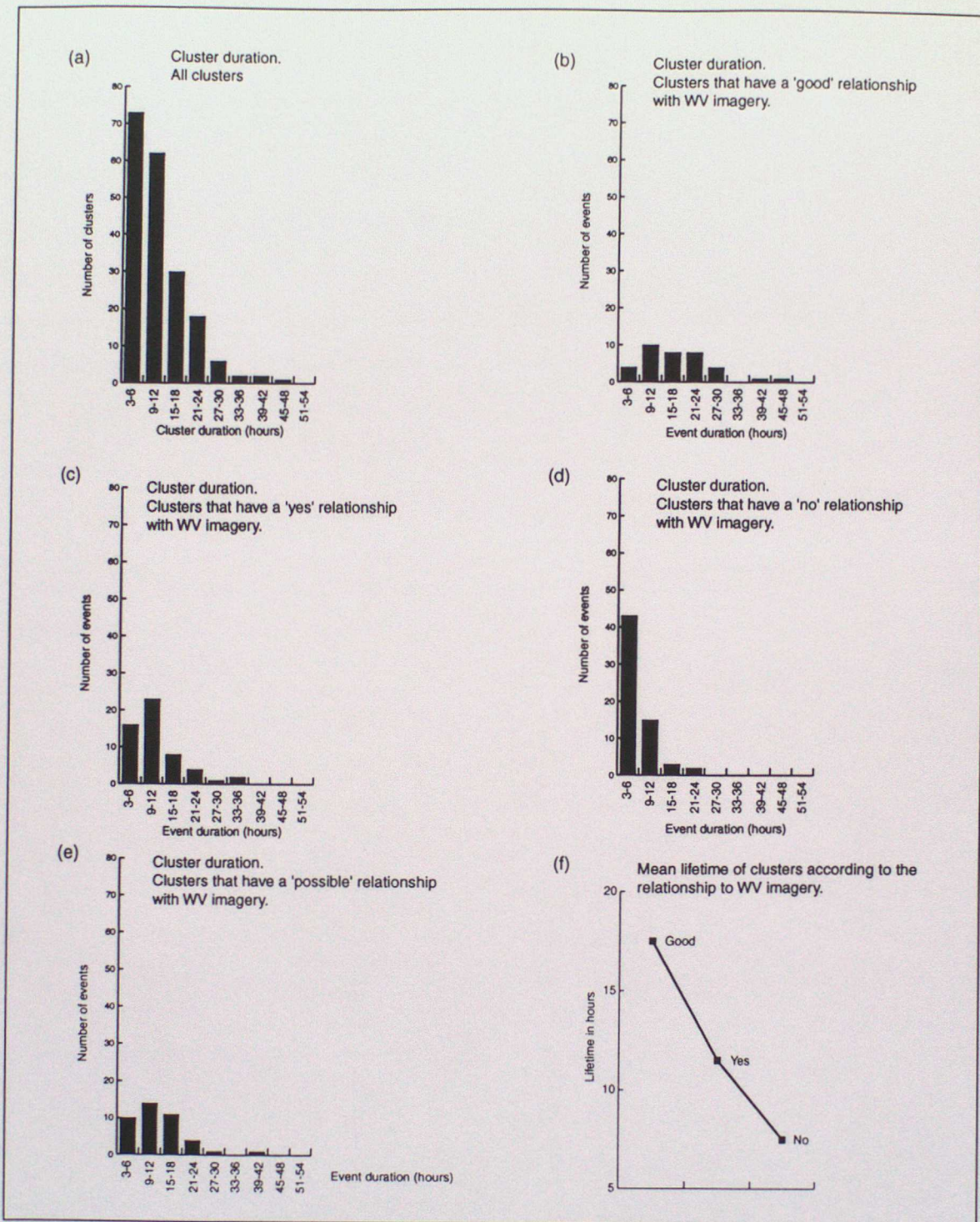


Figure 10.

Of greater interest are the bar charts shown in Figures 10(b), (c), (d) and (e) which show, in turn, storm cluster duration for the 'good', 'yes', 'no' and 'possible' relationships with WV imagery. It is immediately apparent that a pattern has emerged. The clusters that had a 'good' relationship with WV imagery have the largest spread in cluster duration; they include the clusters that persist the longest (some longer than 24 hours) and only a few fall into the smallest duration 3-6 hour bin.

The clusters that had a 'no' relationship with WV imagery have the smallest spread in cluster duration; none of these clusters persist for longer than 24 hours and the most populated bin, by far, is the smallest duration of 3-6 hours. The 'yes' relationship category has a distribution that lies between the other two. For completeness the 'possible' relationship category is also displayed and shows a distribution similar to the 'yes' relationship.

To complete the picture, the difference in mean lifetime between clusters with a 'good', 'yes' and 'no' relationship with WV imagery is shown in Figure 10(f). The results appear to show that storm clusters which have a 'good' relationship with WV imagery persist on average for twice as long as clusters that have no relationship with the imagery.

It is possible to suggest an explanation for these results. Clusters that have a 'no' relationship with WV imagery are likely to have been triggered by low-level effects such as surface heating, low-level convergence, sea-breeze fronts or local orography. The lifetimes of such storms are therefore likely to be strongly controlled by the diurnal cycle, especially in summer when most storms are triggered over land (see Figure 11(b)). Indeed, only 7% of 'no' relationship clusters persisted beyond midnight, compared to 49% of the 'good' and 'yes' clusters. Clusters that have a relationship with WV imagery can be maintained by the dynamical processes signified by the imagery and are therefore less likely to switch off when solar heating stops. This is not to say that surface effects do not play an important role in the imagery-related storms. The large increase in mean lifetime from 'yes' to 'good' is curious. It suggests that the subjective assessment of the cluster-imagery relationship is a guide to the strength of the upper-level forcing. In other words; the clearer the WV-imagery relationship the stronger the upper-level forcing and the longer the storm cluster persists (also assuming that the duration of storms is related to the strength of the upper-level forcing).

3.2.2 Summer period, storm cluster severity (Figure 11)

Figure 11(a) shows that around 1/5th of the storm clusters were severe and the remaining 4/5ths were equally split between medium and weak. This definition of storm intensity does have drawbacks; just because the weak storm clusters had smaller dimensions or fewer lightning reports or were more scattered does not necessarily mean that they were not locally very intense. However, the measure of lightning intensity used here does probably reflect reasonably well the larger scale severity and organisation of the storm clusters.

The grouping of the severe clusters according to their relationship to WV imagery is shown in Figure 11(c). The percentages are out of the total for the individual relationship type rather than out of the whole total: i.e. Figure 11(c) shows that 42% of the 'good' relationship clusters were severe, NOT that 42% of severe clusters had a 'good' relationship. It is clear, that the better the relationship with WV imagery the greater the proportion of severe storm clusters. The pattern is much the same when examining severe and medium clusters together (Figure 11(d)). A striking result from Figure 11(d) is that 86% of the 'good' relationship clusters were either severe or medium in intensity.

Another approach is to calculate the percentage of the severe clusters that have a WV imagery relationship. There is no bar chart to show this, but the key results are:

58% of severe storm clusters had a 'good' or 'yes' relationship with WV imagery
13% of severe storm clusters had no relationship with WV imagery

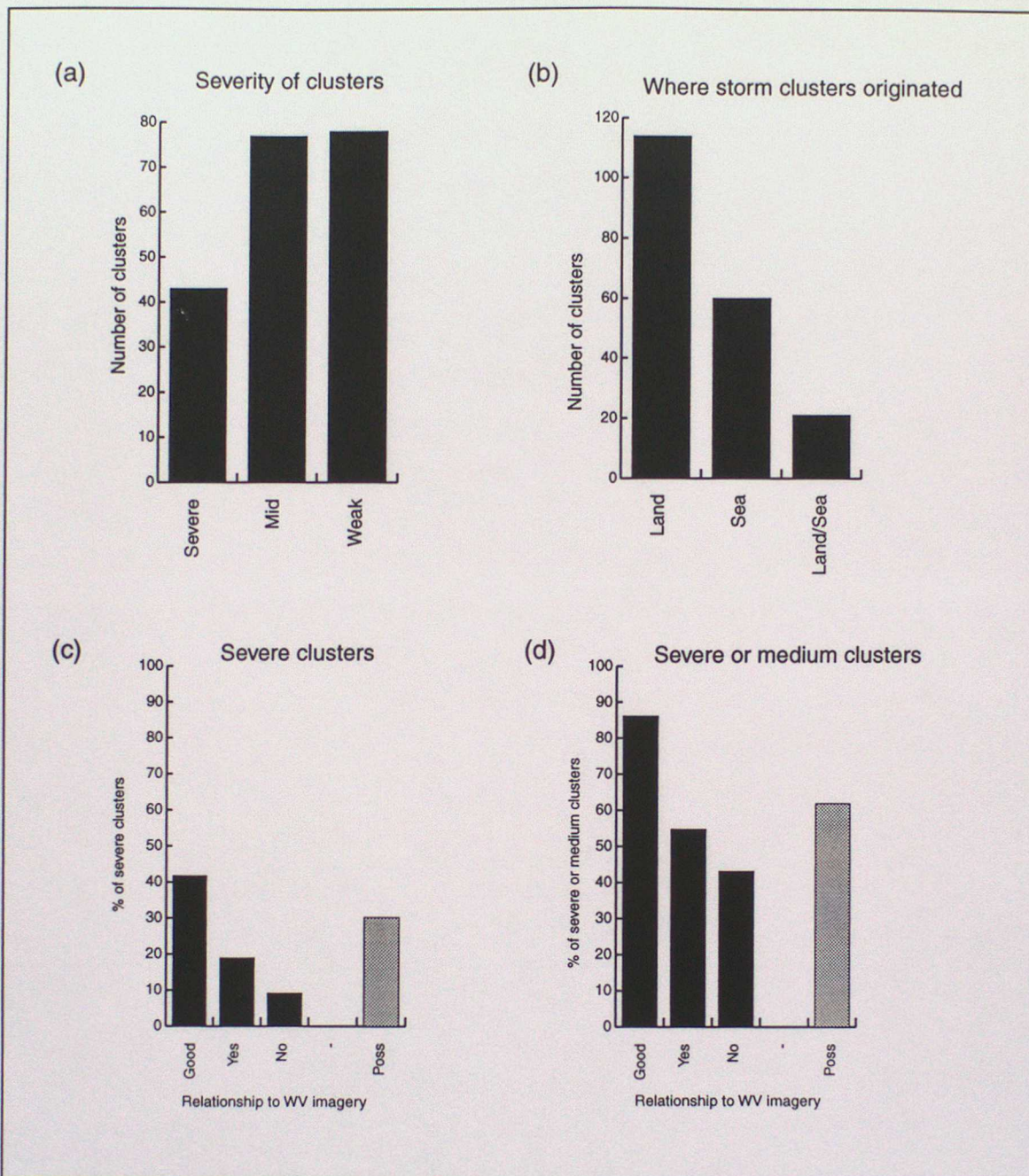


Figure 11.

3.3 Results from the autumn study (Figures 12, 13 & 14)

Much of the results from the autumn study are very similar to the summer study. The discussion here will be focussing on the similarities and differences between the two periods rather than repeating what has already been covered.

Number of days with data	47	
Number of clusters	111	(2.4 clusters per day)

The key results from Figure 12

- 63% of storm clusters (excluding 'possibles') showed a relationship with WV imagery
- 74% of days had a storm cluster related to WV imagery in the domain
- 33% of the storm clusters do not have a relationship with WV imagery

These figures are remarkably similar to the summer study. The only difference is that the proportion of clusters that had a relationship with WV imagery has gone up from 58% to 63%.

A much smaller proportion of the clusters had a 'possible' relationship with WV imagery in the autumn compared with the summer. This could be because of the greater experience in interpreting the imagery, but it is mostly likely that WV-imagery signatures are clearer in the autumn as a result of there being fewer large storms over land and consequently less cirrus outflow to obscure dry zones and complicate the picture.

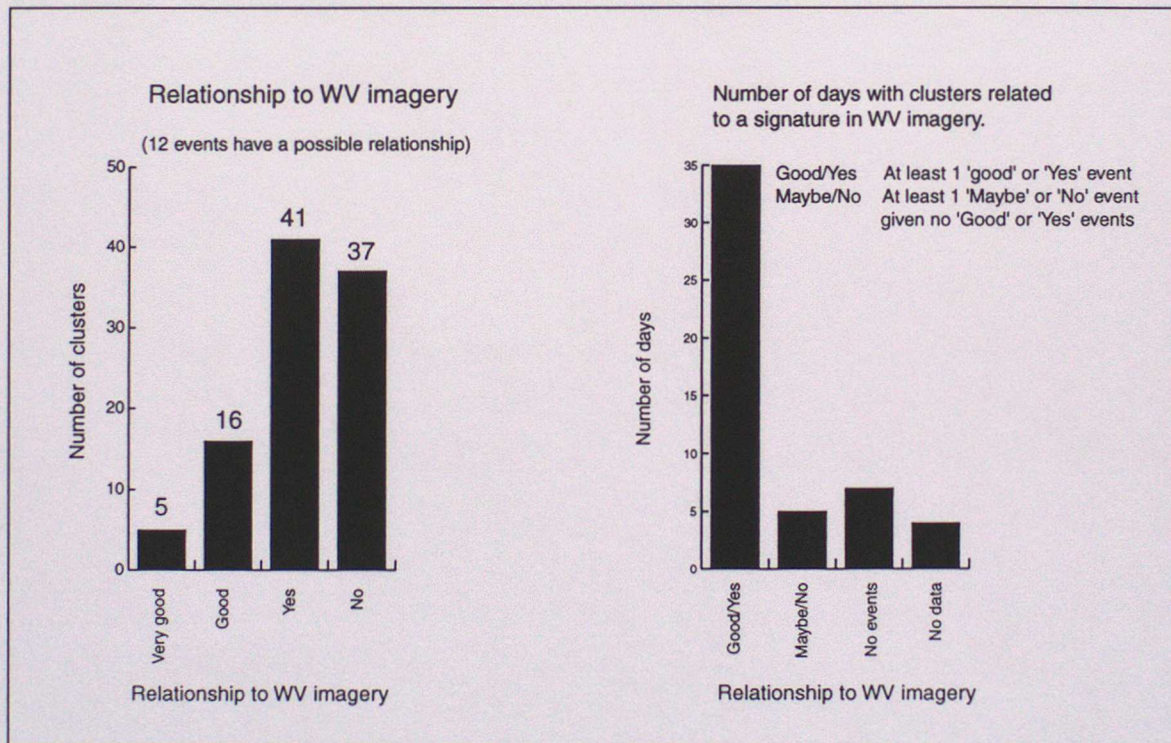


Figure 12.

3.3.1 Autumn study, storm cluster duration (Figure 13)

Figure 13 reveals that the distribution patterns of storm cluster duration in the autumn are very similar to the summer for the various relationships with WV imagery. The only difference is that the autumn clusters have a systematically longer average duration for all relationships with imagery (Figure 16(f)). We might expect intuitively that the converse would be true and summer storms would persist longer. A variety of reasons may explain the difference. It could be that the result is invalid because the autumn sample in particular is quite small and the average difference

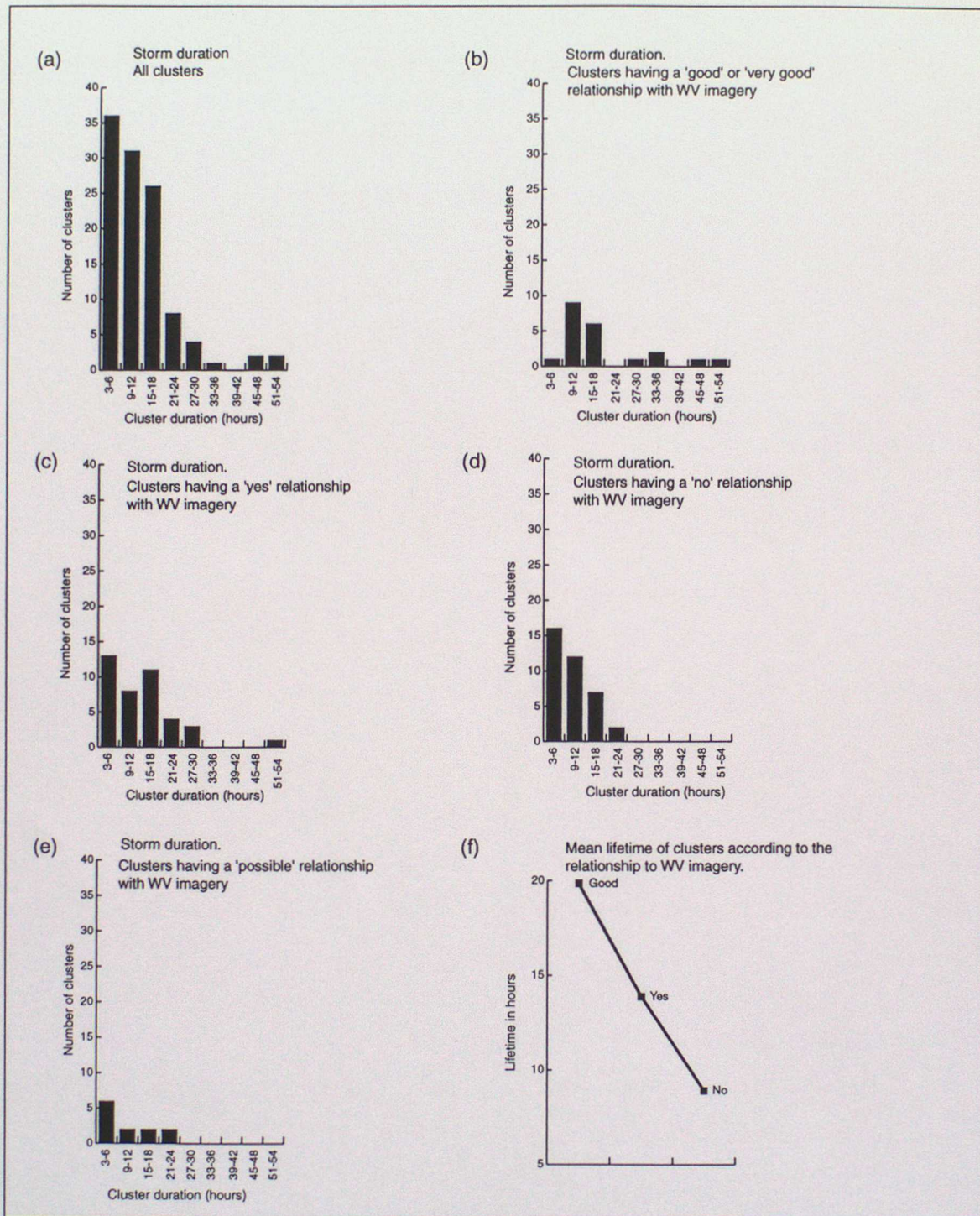


Figure 13.

is only a couple of hours, when the measurements for each cluster were only made to the nearest 3 hours. The only way to assess if the seasonal difference is real is to include many more clusters in the database. In spite of this, let us just suppose, for now, that the difference is real and make a guess at why. A difference between summer and autumn conditions that immediately springs to mind is the intensity of solar heating. It is therefore probable that the summer clusters, especially those with a 'no' relationship with the imagery' would be more controlled by the diurnal cycle.

This is supported by figures from the studies; 30% of the 'no' relationship clusters in autumn persist beyond midnight compared to the 7% in summer. Another significant difference between the summer and autumn clusters is that a much higher proportion form over land in the summer and over the sea in the autumn (see Figures 11(b) & 14(b)). Storms that form over the sea in autumn have access to a constant store of energy, which is not modulated by the diurnal cycle. The sea surface in autumn is still warm: cooling only slowly after the summer. In addition, autumn is the time of year when the North Atlantic storm track becomes more active and major excursions of colder air from the north over the warm sea, are more common. A more active storm track is also coupled with a stronger jet stream, stronger upper-level dynamical forcing and more 'active' dry intrusions in WV imagery.

Although storms may appear to persist longer in the autumn period, it should be remembered that there are fewer of them (especially over land) and storm activity at any one time is still greater in the summer.

3.3.2 Autumn period, storm-cluster severity (Figure 14)

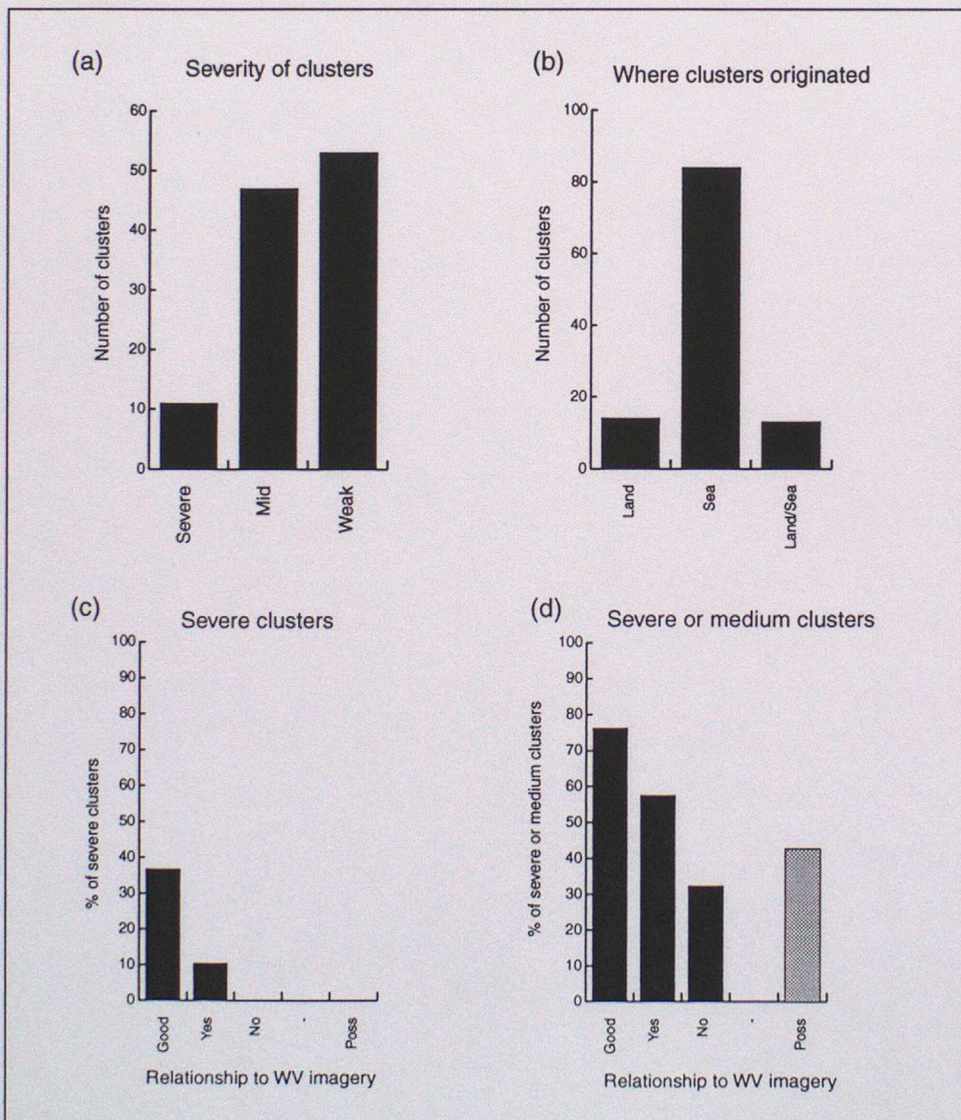


Figure 14.

Unsurprisingly, there was a much smaller proportion of severe storm clusters in autumn than in summer (Figures 11(a) and 14(a)). Of the severe storms that did occur in autumn, every single one was related to a dry zone in WV imagery. The sample was small, (only 11 severe clusters in autumn), but this does suggest that thunderstorms in autumn are only likely to be severe (according to the criteria in this study) if there is sufficient upper-level forcing and advected potential instability to trigger and maintain them.

3.4 Combined results

3.4.1 Classification of the relationship to WV imagery

Each of the thunderstorm clusters that had a relationship with WV imagery was classified according to the type of relationship under the categories presented in section 2.

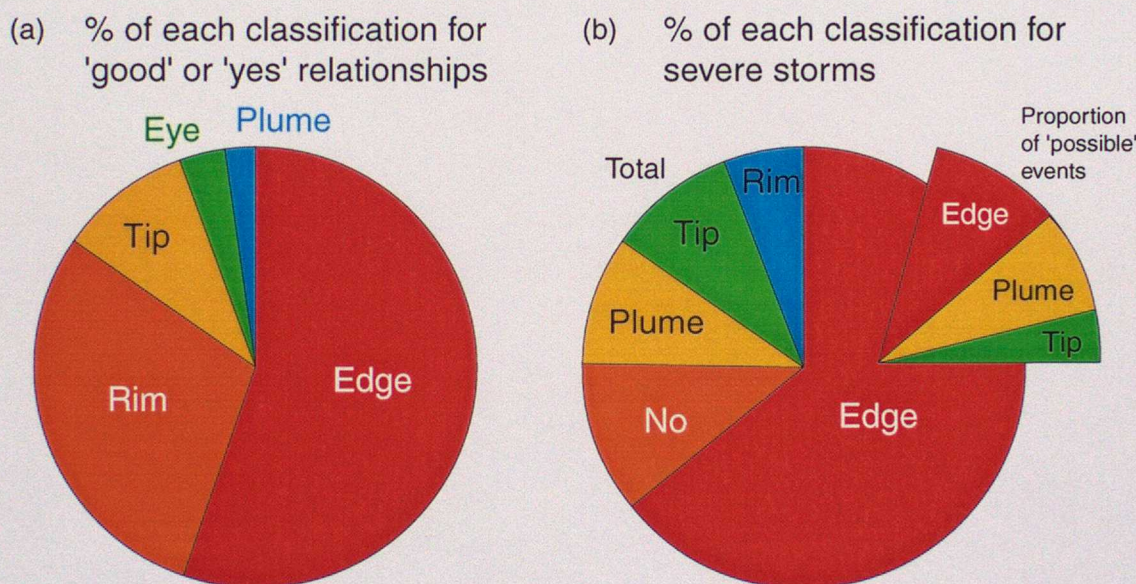


Figure 15

Figure 15(a) shows that over half of the events with a relationship were classed as 'dry edge' and most of the remainder as 'dry arc'. Only a small proportion were 'dry eye' or 'dry plume'. It is not surprising that only a few were 'dry plume' because such events are associated with one particular synoptic pattern and even if that pattern occurs the thundery breakdown is often classed as a 'dry edge' event. It is more surprising that the 'dry eye' category accounts for so few events given the quality of the examples in Section 2. There are two possible explanations for this. Firstly, the distinction between 'dry eye' and 'dry edge' is somewhat arbitrary (to do with scale, aspect ratio and baroclinicity) and some of the dry-edge events could be classed as 'dry eye'. Secondly, many of the dry eye events are weak in terms of number of spheres and do not meet the criteria for this study, even though they may account for a significant number of convective events.

Figure 15(b) shows that nearly two thirds of all the severe storm events were classed as occurring on a dry edge (including 'possible' relationship events). Only around 10% of all severe storms did not have a relationship with WV imagery. Most of the 'dry plume' category severe events were

classified as having a 'possible' relationship with WV imagery. This is because it was not usually reasonable to relate individual storm clusters to the broad-scale nature of the 'dry plume' pattern.

3.4.2 Storm cluster duration

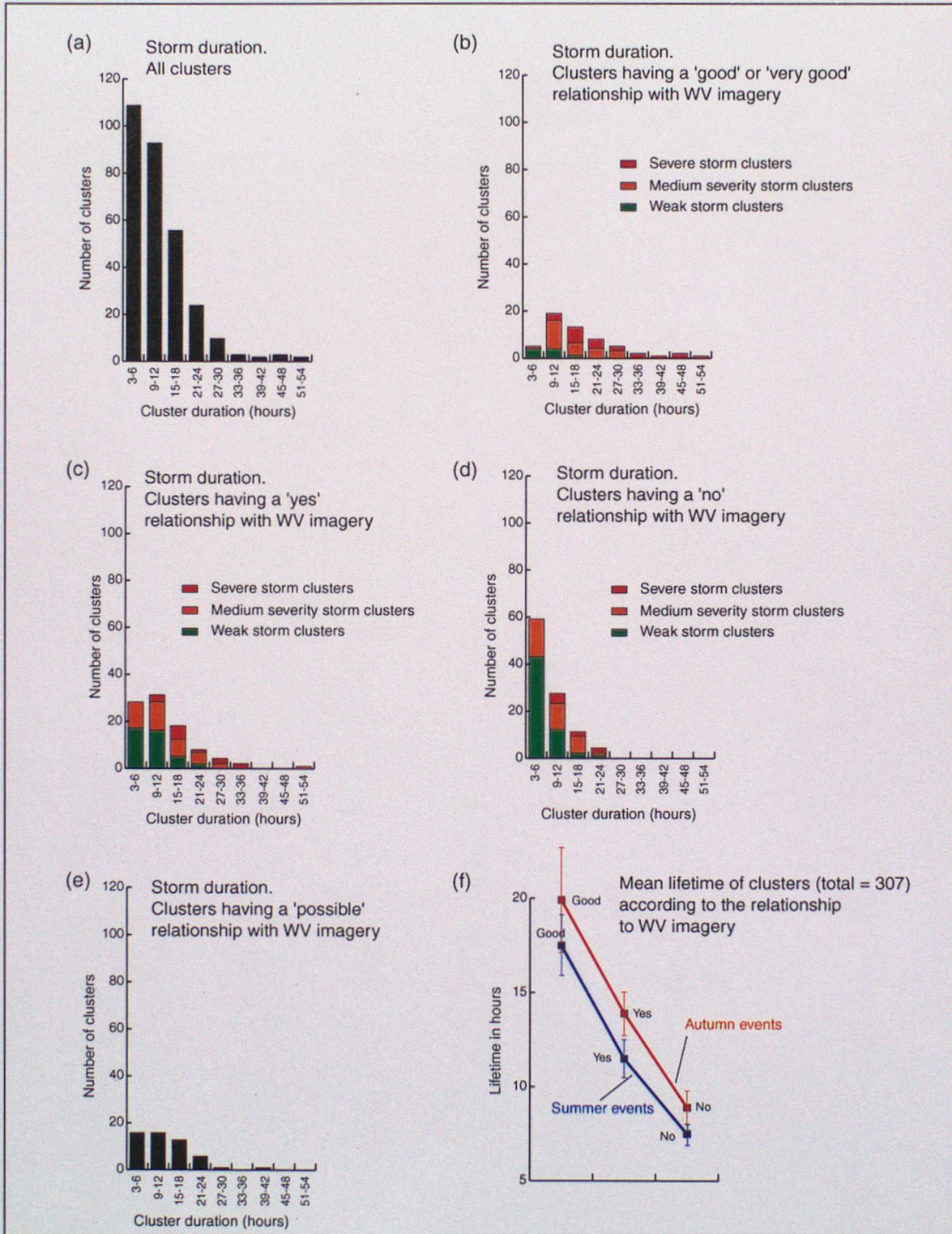


Figure 16

Figure 16(a-e) combines the summer and autumn data for storm cluster duration to show the distributions for the 'all', 'good', 'yes', 'possible' and 'no' relationship categories. An increased number of events results in more smoothly varying distributions. Figure 16(f) shows the apparent increased duration of storm clusters in autumn than winter, as discussed in section 4.3.1. The general trend towards the more severe events having a better relationship with the imagery and longer duration is highlighted by the bar colour split in (b), (c) and (d).

3.4.3 Key results from the combined studies

- Thunderstorms that are related to WV imagery dry regions are common.
 - 60% of storm clusters (excluding 'possibles' from the statistics) showed a relationship with WV imagery
 - At least half of all thunderstorm events (including 'possibles' in the statistics, but not as having a relationship) were related to WV imagery dry regions
 - 74% of days had a storm cluster related to WV imagery in the domain
 - Over 80% of severe thunderstorm events had a WV imagery signature
- On average, thunderstorm clusters that were related to WV dry regions persisted for 4-10 hours longer than thunderstorm clusters with no WV imagery relationship (although the spread is large).

If a storm cluster is related to WV imagery there is a 44% likelihood that it will persist longer than 12 hours, compared to 14% if the storm cluster is not related to the imagery.

If a severe storm cluster is related to WV imagery there is an 86% likelihood that it will persist longer than 12 hours (35% for over 24 hours), compared to 50% (<5%) if the severe storm cluster is not related to the imagery.

- The 'dry edge' relationship with WV imagery is the most common of the categories, especially for the more severe events.

4. Conclusions

Overview

Thunderstorms frequently occur in preferred locations at the edges of, or beneath, dry/dark (high brightness temperature) regions seen in WV imagery. In a study spanning two seasons, of more than three hundred thunderstorm events over Western Europe and the North Atlantic, more than 50% of the thunderstorm events were clearly related to dry/dark regions in the imagery. When removing from the statistics the undecided category containing events having a 'possible' relationship with the imagery, the proportion of events related to the imagery increased to 60%. The results indicate that the more severe a thunderstorm event is or the longer it persists the better the relationship with WV imagery is likely to be.

Dry regions in WV imagery primarily reveal where there is a local lowering of the tropopause. Such tropopause depressions (or folds) are generally associated with an upper-tropospheric high-PV anomaly, vertical motion with ascent ahead and descent behind the PV anomaly and relatively low- θ_w air in the mid troposphere. Thunderstorms occur when potential instability can be generated (by differential advection or surface heating) and then released where there is sufficient dynamical ascent or surface heating. WV imagery therefore provides a guide to where thunderstorms may develop by indicating where the most favourable dynamical conditions are likely to be.

A number of examples have been used to show the relationship between thunderstorm events and dry regions in WV imagery. Each of these examples fits into one of six categories - 'dry eye', 'dry edge', 'inner crescent rim', 'dry tip', 'dry plume' and 'orographic'. The difference between each of these categories is based on the shape and size of the dry region and the location of thunderstorms relative to that dry region. Although there is some overlap, each category represents a distinctive atmospheric flow pattern and convection triggering mechanism. 'Dry eye' thunderstorms occur ahead of and beneath almost circular or lens shaped dry regions that are associated with isolated upper-level vorticity anomalies. 'Dry edge' thunderstorms occur at the leading edge of dry regions that are associated with the baroclinic zone and vorticity at the forward edge of upper-level troughs. 'Inner crescent rim' thunderstorms occur along the cold-air side fringe of the crescent-shaped dry regions that mark the base and edge of upper-level troughs. 'Dry tip' thunderstorms are found at the northern tip of long stretched dry regions in a location where there is vorticity and ascent. 'Dry plume' thunderstorms are associated with mid-level convective instability within poleward advecting plumes of warm air ahead of upper-level troughs. 'Orographic' thunderstorms occur where orographic uplift releases any potential instability beneath a dry region. This split into categories is useful. It provides a basis for breaking down a complex WV image into the important components and on many occasions allows an instant visual diagnosis of the dominant dynamical forcing mechanism that may be associated with a convective event.

This report has presented a study showing the proportion of thunderstorms that are associated with dry intrusions, but not the proportion of dry intrusions that are associated with thunderstorms - this still requires investigation.

Recommendations for Forecasting

The relationship between WV imagery and thunderstorms should be developed as an important additional tool in the operational forecasting of deep convection. The information could be applied in three ways.

(1) To detect numerical model analysis and forecast errors. A mismatch in location between an upper-level vorticity anomaly in the numerical model and a dry zone in the imagery allows a way to determine whether any convection associated with the vorticity anomaly is likely to be misplaced (see dry edge thunderstorms -example 4). Such a comparison is most useful for smaller-scale features (<300km across). They tend to have a more simple structure that more exactly relates to the imagery than the larger-scale troughs or cyclones and are more likely to be incorrectly positioned or missed altogether in a numerical model analysis.

(2) To deduce 'risk' regions where deep convection or thunderstorms are more likely to occur, or where showers are more likely to be thundery. A 'risk' region will of course vary in size and certainty according to the characteristics of a particular dry zone in the imagery and on other factors relevant to the particular situation. There are however occasions when a well-defined pattern in the imagery will clearly focus the risk on a small area where thunderstorms are highly likely. Probability based forecasts of risk areas could be constructed for up to 12 hours ahead, based on a combination of WV imagery, numerical model output and the evaluation of numerical model error based on the imagery.

(3) To determine the likely future behaviour of existing thunderstorms on the basis of whether they are largely dynamically forced or surface driven. Thunderstorms associated with a vorticity signature in WV imagery tend to move with the mid-tropospheric flow; they persist longer and are less constrained by the diurnal cycle over land than locally forced or open cellular convection.

To make the best use of WV imagery requires training and good display facilities. Training is essential, as interpretation of WV imagery in this regard is a skill that must be acquired. A graphical display system must be able to display and animate WV imagery in colour as well as grey shade and have the capability of overlaying sferics, radar and key numerical model output fields. The most essential diagnostic fields for comparison with WV imagery are 500hPa vorticity (this usually correlates well with smaller-scale vorticity signatures in WV imagery) and a pseudo WV image diagnostic that calculates an equivalent to what the WV channel 'sees'. Vorticity (or PV) at 300hPa should be used in conjunction with the 500hPa vorticity field to determine vertical structure.

High-resolution numerical models

As computer power increases so the resolution of numerical forecast models improves. There is a common perception that the prediction of convection will improve as factors such as local orographic effects, boundary layer convergence and local 'heat islands' become better represented. While this may be true, the results in this report strongly suggest that over half of all thunderstorm events are associated with dynamical forcing through the depth of the troposphere at scales that can be resolved by models with a horizontal grid spacing of 20km or better. In these situations the performance of convective or boundary layer schemes may be of secondary importance. The benefit of continuing to go to higher resolution for predicting convective events needs to be assessed, both for those events where local effects and processes dominate and for the events where the resolved-scale dynamical forcing is the driving mechanism.

Numerical model sensitivity experiments

WV imagery provides an independent way of identifying which convective events are clearly associated with an upper-level vorticity anomaly. The accuracy of forecasts of these events can be assessed and categorised on the basis of a comparison of the resolved-scale dynamics with the imagery along with a comparison of the forecast precipitation pattern with radar data. The good forecasts of clear-cut dynamically forced events should be extremely valuable for model sensitivity experiments, because the forcing mechanism is known and captured by the model. These cases can be used to investigate the performance of high-resolution versions of the Unified Model by testing the resolved and convective responses to modifications such as changing the horizontal and vertical resolution, dynamics formulation or convective parametrization. The bad forecasts can be split into two categories, either the resolved-scale dynamics is wrong or the resolved-scale dynamics is reasonable but the convection is wrong. The first of these categories encompasses situations where the upper-level vortex inferred from the imagery is either absent or badly misplaced in the model. In many instances this will be largely a data assimilation issue. Such cases could be valuable for testing new data assimilation schemes or trying new methods for modifying a model analysis, such as the assimilation of a vorticity operator or the use of PV inversion techniques. The category of cases where the convection is poorly forecast in relation to apparently good resolved-scale dynamical forcing is more complex because many factors could account for the error, nevertheless experiments to try and improve these forecasts should still provide valuable insight.

VAR & MSG

With the introduction of 3D and 4DVAR data assimilation, direct assimilation of WV imagery becomes possible and the impact of this development in terms of the skill in the prediction of deep organised convection needs to be assessed. The new Meteosat Second Generation (MSG) satellite will have two WV channels, improved resolution and images every 15 minutes. This opens up the opportunity to develop an improved understanding of the relationship between WV imagery and thunderstorms that should eventually result

in an extremely valuable product for forecasting, high-resolution modelling and data assimilation.

5. Acknowledgements

I wish to thank to Peter Clark and Prof. Keith Browning for their comments on the scope and content of earlier drafts of this report, which have resulted in significant improvements. I am grateful to Prof. Keith Browning for sharing his considerable knowledge and insight over a number of years. None of this work could have been done without the JCMM display program DISP, which was initially developed by Dr. Sid Clough, developed further by Tim Hewson and maintained by Andy Macallan.

6. References

- Browning, K.A., 1993: Evolution of a mesoscale upper tropospheric vorticity maximum and comma cloud from a cloud-free two-dimensional potential vorticity anomaly. *Quart.J.Roy.Meteor.Soc.*, 119, 883-906
- Browning, K.A. and B.W. Golding, 1995: Mesoscale aspects of a dry intrusion within a vigorous cyclone. *Quart.J.Roy.Meteor.Soc.*, 121, 463-493
- Browning, K.A. and G.A. Monk, 1982: A simple model for the synoptic analysis of cold fronts. *Quart.J.Roy.Meteor.Soc.*, 108, 435-452
- Browning, K.A. and N.M. Roberts, 1994: Use of satellite imagery to diagnose events leading to frontal thunderstorms. Part I of a case study. *Meteorol.Appl.* 1, 303-310.
- Browning, K.A. and N.M. Roberts, 1995: Use of satellite imagery to diagnose events leading to frontal thunderstorms. Part II of a case study. *Meteorol.Appl.* 2, 3-9.
- Browning, K.A., N.M. Roberts and C.S. Sim, 1996: A mesoscale vortex diagnosed from combined satellite and model data. *Meteorol.Appl.*, 3, 1-4
- Carr, F.H. and J.P. Millard, 1985: A composite study of comma clouds and their Association with severe weather over the Great Plains, *Mon. Wea. Rev.*, 113, 370-387

- Danielsen, E.F., 1964: Project Springfield Report. Defense Atomic Support Agency, Washington D.C. 20301 DASA 1517 (NTIS # AD-607980), 97 pp.
- Griffiths, M., A.J. Thorpe and K.A. Browning, 1998: Convective destabilisation by a tropopause fold diagnosed using potential vorticity inversion. JCMM internal report, 96
- Hobbs, P.V., J.D. Locatelli, and J.E. Martin 1990: Cold fronts aloft and the forecasting of precipitation and severe weather east of the Rocky Mountains. *Wea.Forecasting*, 5, 613-626.
- Hoskins, B.J., M.E. McIntyre and A.W. Robertson, 1985: On the use and significance of isentropic potential vorticity maps. *Quart.J.Roy.Meteor.Soc.*, 111, 877-946.
- Lee, A.C.L., 1989: Ground truth confirmation and theoretical limits of an experimental VLF arrival time difference lightning flash location system. *Quart.J.Roy.Meteor.Soc.*, 115, 1147-1166.
- Ludlam, F.H., 1980: Clouds and Storms: The Behaviour and Effect of Water in the Atmosphere. The Pennsylvania State University Press. 405pp.
- Parker, D.J., 1999: Passage of a tracer through frontal zones: A model for the formation of forward-sloping cold fronts. *Quart.J.Roy.Meteor.Soc.*, 125, 1785-1800.
- Roberts, N.M., 1995: Association of sferics with a dry intrusion in Meteosat imagery. *Meteorol.Appl.* 2, 109-111.
- Roberts, N.M., 2000: A guide to aspects of water vapour imagery interpretation: the significance of dry regions. JCMM internal report, 109
- Thorncroft, C.D., B.J. Hoskins and M.E. McIntyre, 1993: Two paradigms of baroclinic-wave life-cycle behaviour. *Quart.J.Roy.Meteor.Soc.*, 119, 17-55.
- Young, M.V., G.A. Monk and K.A. Browning, 1987: Interpretation of satellite imagery of a rapidly deepening cyclone. *Quart.J.Roy.Meteor.Soc.*, 113, 1089-1115